eNeuro

Research Article: New Research | Integrative Systems

Parallel Arousal Pathways in the Lateral Hypothalamus

Jaime E. Heiss[1], Akihiro Yamanaka[2] and Thomas S. Kilduff[1]

[1]*Biosciences Division, Center for Neuroscience, SRI International, Menlo ParkCA 94025, USA*
[2]*Department of Neuroscience II, Res. Inst. of Environmental Medicine, Nagoya University, Nagoya Japan*

DOI: 10.1523/ENEURO.0228-18.2018

Received: 7 June 2018

Revised: 11 July 2018

Accepted: 12 July 2018

Published: 1 August 2018

Author Contributions: JH designed research, performed research, contributed unpublished reagents/ analytic tools, analyzed data and wrote the paper. AY designed research and contributed unpublished reagents/ analytic tools. TK designed research, contributed unpublished reagents/ analytic tools and wrote the paper.

Funding: http://doi.org/10.13039/100000065HHS | NIH | National Institute of Neurological Disorders and Stroke (NINDS)
R01NS077408
R01NS098813

Funding: KAKENHI, MEXT, Japan
16H01271
15H01428

Conflict of Interest: Authors report no conflicts of interest.

Research was supported by R01NS077408 and R01NS098813 from the National Institutes of Health and by KAKENHI grants (16H01271, 15H01428 to A.Y.) from Ministry of Education, Culture, Sports Science, MEXT, Japan. The content is solely the responsibility of the authors and does not necessarily represent the official views of the National Institutes of Health.

Corresponding author: Thomas S. Kilduff, 333 Ravenswood Ave, Menlo Park, CA 94025. E-mail: thomas.kilduff@sri.com

Cite as: eNeuro 2018; 10.1523/ENEURO.0228-18.2018

Parallel Arousal Pathways in the Lateral Hypothalamus

Abbreviated Title: Parallel hypothalamic arousal mechanisms

Authors: Jaime E. Heiss[1], Akihiro Yamanaka[2], Thomas S. Kilduff[1]

[1]Center for Neuroscience, Biosciences Division, SRI International, Menlo Park, CA, 94025 USA

[2]Dept. of Neuroscience II, Res. Inst. of Environmental Medicine, Nagoya Univ., Nagoya, Japan

Author Contributions: JH designed research, performed research, contributed unpublished reagents/ analytic tools, analyzed data and wrote the paper. AY designed research and contributed unpublished reagents/ analytic tools. TK designed research, contributed unpublished reagents/ analytic tools and wrote the paper

Corresponding author: Thomas S. Kilduff (thomas.kilduff@sri.com). 333 Ravenswood Ave, Menlo Park, CA 94025

Figures: 8, **Tables**: 2

Pages: 46 **Figures**: 8 **Tables**: 2

Number of words in Abstract: 249, Significance: 91, Introduction: 615, Discussion: 1,511

Acknowledgements: We thank Dr. Michael Schwartz for comments on the manuscript, Dr. Ling Jong for almorexant synthesis and Messrs. Webster Lincoln, Jeremiah Palmerston and Gabriel Orellana, as well as Ms. Deepti Warrier and Ms. Jennifer Walters for technical assistance.

Authors report no conflicts of interest.

Funding Sources: Research was supported by R01NS077408 and R01NS098813 from the National Institutes of Health and by KAKENHI grants (16H01271, 15H01428 to A.Y.) from Ministry of Education, Culture, Sports Science, MEXT, Japan. The content is solely the responsibility of the authors and does not necessarily represent the official views of the National Institutes of Health

Abstract

Until recently, hypocretin (Hcrt) neurons were the only known wake-promoting neuronal population in the lateral hypothalamus (LH), but subpopulations of inhibitory neurons in this area and glutamatergic neurons in the nearby supramammillary nucleus (SuM) have recently been found that also promote wakefulness. We performed chemogenetic excitation of LH neurons in mice and observed increased wakefulness that lasted more than 4h without unusual behavior or EEG anomalies. The increased wakefulness was similar in the presence or absence of the dual orexin receptor blocker almorexant (ALM). Analysis of hM3Dq transfection and c-FOS expression in LH inhibitory neurons and in the SuM failed to confirm that the increased wakefulness was due to these wake-promoting populations, although this possibility cannot be completely excluded. To evaluate the relationship to the Hcrt system, we repeated the study in *Orexin-tTA* mice in the presence or absence of dietary doxycycline (DOX), which enabled us to manipulate the percentage of Hcrt neurons that expressed hM3Dq. In DOX-fed mice, 18% of Hcrt neurons as well as many other LH neurons expressed hM3Dq; these mice showed a profound increase in wake after hM3Dq activation even in the presence of ALM. In mice switched to normal chow, 62% of Hcrt neurons expressed hM3Dq along with other LH cells; chemogenetic activation produced even more sustained arousal which could be reduced to previous levels by ALM treatment. Together, these results indicate an LH neuron population that promotes wakefulness through an Hcrt-independent pathway that can act synergistically with the Hcrt system to prolong arousal.

Visual Abstract

Activation of lateral hypothalamic (LH) neurons transfected with hM3Dq (denoted in blue) induces profound Hcrt-independent wakefulness (% W) that can further increase after activation of Hcrt signaling pathways, suggesting the existence of independent, parallel wake-promoting mechanisms in LH. Arrows denote injection of either vehicle (VEH) or the dual Hcrt receptor antagonist almorexant (ALM) at ZT4 and either CNO or saline at ZT5.

Significance

Despite nearly a century of evidence suggesting that the lateral hypothalamus contains neurons essential to sustain wakefulness, the primary wake-promoting cells in this brain region studied to date have been the hypocretin/orexin neurons. Here, we show that chemogenetic excitation of lateral hypothalamus neurons can induce sustained wakefulness even in absence of hypocretin signaling and that concurrent hypocretin neuron activation can prolong arousal. These results indicate the existence of parallel arousal pathways in the lateral hypothalamus and suggest a new therapeutic target for disorders of excessive sleepiness such as hypersomnia and narcolepsy.

Introduction

The lateral hypothalamus (LH) has been thought to play a critical role in sleep-wake regulation since the early studies of Von Economo (Von Economo, 1930). Lesions and acute inhibition of LH neurons are known to increase sleep time (Ranson, 1939; Nauta, 1946; de Ryck and Teitelbaum, 1978; Shoham and Teitelbaum, 1982; Cerri et al., 2014) while excitation produces arousal and increases in activity (Krolicki et al., 1985; Sinnamon et al., 1999; Alam and Mallick, 2008; Li et al., 2011). Several studies have identified wake-active neurons in the LH (Alam et al., 2002; Koyama et al., 2003; Lee et al., 2005) but their neurochemical identity is unknown. More recently, inhibitory LH neuronal populations have been identified that induce wakefulness upon optogenetic or chemogenetic stimulation (Herrera et al., 2016; Venner et al., 2016). The wake-promoting LH cell population that has been studied most extensively to date are the hypocretin/orexin (Hcrt) neurons (de Lecea et al., 1998; Peyron et al., 1998; Kilduff and Peyron, 2000; Gerashchenko et al., 2001; Bonnavion and de Lecea, 2010). These cells project to several wake-promoting areas of the brain including the basal forebrain (BF), the tuberomamillary nucleus (TMN) and the locus coeruleus (LC) where they can release the Hcrt peptides, glutamate, dynorphin and perhaps other neurotransmitters (Torrealba et al., 2003; Eriksson et al., 2004; Schone et al., 2012; Schone et al., 2014). In this regard, the Hcrt neurons have been proposed to act like a stabilizer of a flip-flop switch that controls behavioral state (Saper et al., 2005).

Narcolepsy is a neurological disease characterized by the extensive loss of Hcrt neurons without degeneration of neighboring cells (Kilduff and Peyron, 2000; Thannickal et al., 2000). Narcoleptic patients are unable to sustain long periods of consolidated wakefulness and must

nap frequently; some patients also experience attacks of cataplexy which greatly affects their quality of life (Kornum et al., 2017). However, total sleep time in untreated narcoleptic patients as well as in mouse models of narcolepsy does not differ from controls over the 24h period (Dantz et al., 1994; Hara et al., 2001; Tabuchi et al., 2014), a phenotype that is distinct from the lethargy observed after LH lesions or acute LH neuronal inhibition. Chemogenetic excitation of Hcrt neurons in mice (Sasaki et al., 2011) produced a 30% increase in wake time during the first hour of stimulation compared to controls but no significant difference was observed after the second hour, which also differs from the effects of LH excitation cited above. Thus, Hcrt neuron stimulation and ablation studies do not fully recapitulate the effects on wake and sleep observed after manipulations of LH neuron activity, indicating that there are likely other wake-promoting neuronal populations in the LH that may be involved in sleep/wake regulation.

To determine whether LH stimulation has wake-promoting effects distinct from those exhibited by Hcrt neuron stimulation, we performed chemogenetic excitation of LH neurons while conducting EEG and EMG recordings of the transfected mice. We then evaluated the effect of time-of-day on LH-mediated wake promotion and whether Hcrt signaling was necessary to evoke arousal during LH activation. Finally, we combined transfection of LH neurons with a diet-dependent expression of hM3Dq in Hcrt neurons to test whether the Hcrt and non-Hcrt arousal pathways are parallel or overlapping. Our results show that LH neuronal stimulation evokes profound but physiological arousal independent of Hcrt signaling and that concurrent activation of Hcrt and non-Hcrt LH neurons has synergistic effects on arousal that are attenuated in presence of the dual orexin receptor antagonist almorexant (ALM). These results indicate the existence of an LH arousal pathway that can be activated even when Hcrt

signaling is pharmacologically blocked, suggesting a novel target for treatment of sleep/wake disorders such as narcolepsy.

Materials and Methods

Animals. Adult *Gad2-IRES-Cre;R26R-EYFP* (Jax stock # 010802 and 006148; *n* = 6 males and 4 females, 2-4 months old) and *Orexin-tTA* mice (C57BL/6-Tg(orexin/tTA)G5/Yamanaka; *n* = 21 males, 2-4 months old), which express the tetracycline transactivator (tTA) exclusively in the Hcrt neurons (Tabuchi et al., 2014), were singly-housed under a 12h/12h light/dark cycle with *ad libitum* access to food and water in temperature (24 ± 2°C) and humidity (50 ± 20% relative humidity) controlled rooms. 16 of the *Orexin-tTA* mice were reared with chow that included doxycycline (DOX). An additional cohort of C57BL/6J WT mice (Jax stock # 000664; *n =4* males and 4 females, 3-6 months old) were housed under the same conditions and used to assess the effects of clozapine-N-oxide (CNO) treatment on sleep/wake in naïve mice (see Table 1). All studies were conducted in accordance with the Guide for the Care and Use of Laboratory Animals and were approved by the Institutional Animal Care and Use Committee at SRI International. Every effort was made to minimize animal discomfort throughout these studies.

Surgical Procedures. Under isoflurane anesthesia, *Gad2-IRES-Cre;R26R-EYFP* and *Orexin-tTA* mice were injected bilaterally into the LH (-1.4 AP, 1 ML relative to bregma and -5 DV from pia) with 340 nl of an AAV encoding hM3Dq-mCherry (AAV-TetO-hM3Dq-mCherry (Sr10); titer $2x10^{11}$; Nagoya University, Japan) using a Picospritzer II (Parker Instrumentation, Cleveland, OH) connected to a BK Precision 4003A Pulse Generator (B&K Precision Corporation, Yorba Linda, CA) which delivered 5-20 ms pulses of pressurized air every 2 s into a glass

micropipette for 5-10 min. After a recovery period of at least two weeks, injected mice as well as naïve C57BL/6J mice underwent surgery for implantation of EEG and EMG leads by cementing a reference EEG screw over the occipital bone, one in the left frontal bone (1 AP, 1 ML), and another over the parietal bone (-2 AP, 2 ML). EMG electrodes were two stainless steel-coiled wires anchored to the neck musculature. A 5-pin connector was connected to the EEG and EMG leads and cemented to the skull for conventional tethered EEG/EMG recordings.

Experimental Procedures. To allow acclimation to the recording apparatus, mice were connected to a tether that was attached to a commutator (Pinnacle Technology Inc., Lawrence, KS) for at least 5 d prior to experiments. The commutator allowed the mice to move freely in their home cages. For acclimation to the dosing procedure, mice underwent 3 i.p. injections of saline on different days prior to initiation of the dosing study. Experiments occurred no sooner than 21 d after the EEG/EMG implantation surgery. EEG and EMG data were collected at 800 Hz and digitally band-passed at 0.5-300 Hz for *Gad2-IRES-Cre;R26R-EYFP* and WT mice, and at 500 Hz and digitally band-passed at 0.5-200 Hz for *Orexin-tTA* mice using a TDT RZ2 system connected to a 96-channel PZ2 amplifier and a low impedance RA16LI-D headstage (Tucker-Davis Technologies, Alachua, FL). To monitor activity, infrared analog video was collected using CNB B1760N4.3 cameras (CNB Technology Inc., Seoul, Korea) and digitized at 30 fps using a Q-See QT5616 system (Q-See, Anaheim, CA). All animals underwent an undisturbed 24 h baseline recording in their home cages prior to dosing experiments.

Dosing procedures. Clozapine N-oxide (Cat No. 4936, Tocris Bioscience, Avonmouth, UK), the ligand for the modified muscarinic receptor hM3Dq, was injected i.p. at 3 mg/Kg in saline solution at a concentration of 0.5 mg/ml in all experiments. To block Hcrt signaling, the

dual orexin receptor antagonist almorexant (ALM), synthesized at SRI International (Black et al., 2013), was injected i.p. at a concentration of 200 mg/Kg in vehicle (VEH) consisting of 1.25% hydroxypropyl methyl cellulose (SKU 09963), 0.1% dioctyl sodium sulfosuccinate (SKU 323586) and 0.25% methyl cellulose (SKU 274429) in water (all from Sigma-Aldrich, St. Louis, MO) after vortexing a solution of 30 mg/ml for 2 h. Dosing sessions were at least 4 d apart and at least 7 d elapsed between CNO dosings.

In *Gad2-IRES-Cre;R26R-EYFP* mice, dosing occurred either at ZT12 and EEG/EMG was recorded for the subsequent 12 h or at ZT4 and the EEG/EMG was recorded for 9 h starting at ZT3. In *Orexin-tTA* mice, dosing studies were also performed at ZT4 and EEG/EMG was recorded from ZT4 to ZT11. For mice belonging to both the DOX(+) and DOX(-) cohort (n = 10), the DOX-containing chow was replaced by normal chow at least 3 weeks before the dosing study was repeated under the DOX(-) condition.

Locomotor activity data collection and analysis. Synchronization of EEG/EMG data and time-stamped video was achieved by synchronizing the Q-See system's clock to the TDT computer's clock and manually entering the start and end time of all behavioral videos. The position of the mice was detected automatically using Noldus EthoVision XT 11.5 software (Noldus Information Technology, Wageningen, Netherlands). To calculate the speed of the mice in Figs. 3***F,G***, after manually curating the automatic tracking of the mouse's position, we obtained a matrix with the X and Y coordinates of each mouse 30 times/sec as well as a vector with the relative time of each data point. A median filter and then an average filter with a moving window of 10 time points and step of 1 time point was applied to both sets of coordinates and the Euclidean distance with respect to the origin of the coordinate system was

obtained for every time point. The distance traveled was calculated as the absolute value of the difference between the calculated distance and the distance from the first data point. Finally, the speed was calculated as the absolute difference between two consecutive points of the distance travelled, divided by the difference in time between the two consecutive points. All data were processed using custom scripts created in Matlab 2015b (Mathworks, Natick, MA).

EEG/EMG data collection and analysis. Using the criteria described previously (Morairty et al., 2013; Dittrich et al., 2015), EEG/EMG data were visually scored as wake (W), non-rapid eye movement sleep (NREM) or rapid eye movement sleep (REM) in 4 s epochs. A bout of W, NR or REM was defined as three consecutive 4 s epochs (i.e., 12 s) within the same state. For quantitative EEG analysis, the power spectrum was calculated for each 4 s artifact-free epoch using the squared amplitude coefficients of the fast Fourier transform and the mean power in the delta (δ), 0.5-4 Hz; low theta (Lθ), 4-8 Hz; high theta (Hθ), 8-10 Hz; low gamma (Lγ), 15-50 Hz; high gamma (Hγ), 60-80 Hz; and very high gamma (Vhγ), 90-200 Hz range. To avoid 60 Hz artifact, the spectral power values at 60 ± 1 Hz and the harmonics at 120 and 180 Hz were replaced by a linear interpolation from the values at 59 and 61 Hz, 119 and 121 Hz and 179 and 181 Hz. Normalized W power was obtained by dividing the mean power spectrum during W by the mean power in W during the same time period of a baseline recording.

Experimental design and statistical analyses. Table 1 summarizes the 6 dosing experiments that were conducted. Results obtained from male mice were similar to those of female mice and thus data from both sexes were grouped. For statistical analysis, we performed 2-way repeated measures ANOVA using Sigmaplot (Systat Software Inc., San Jose,

CA) followed by Bonferroni-corrected *post hoc t*-tests to identify effects of the different treatments on sleep architecture across time after dosing. To assess sleep rebound effects after the prolonged wakefulness induced by LH neuron activation, we considered all time points following the first hour after dosing when the hourly average NREM sleep time was at least 20%. For comparisons involving only one factor, we used the Matlab function anova1 followed by Tukey's *post hoc* test with Bonferroni correction to identify individual differences between two treatments. To compare the effect of two factors on two different populations, we performed an unbalanced two-way ANOVA using the Matlab function anovan. For estimation of whether two datasets had the same probability distribution, we used the two-sample Kolmogorov-Smirnov goodness-of-fit hypothesis test with the Matlab function kstest2. The Bonferroni correction was also used here for pairwise comparison of more than two distributions. For calculation of Pearson's correlation coefficient (r), we used the Matlab function corrcoef and a significance threshold of $p < 0.05$. To determine the difference between two populations of similar size and estimation of the standard error over the mean associated with a 95% confidence level, we used the formula

$$m_1 - m_2 \pm \frac{\left(z * \sqrt{\frac{s_1^2}{n_1} + \frac{s_2^2}{n_2}}\right)}{\sqrt{\min(n_1, n_2)}}$$

where $z = 1.96$ and m, n and s are the mean, size and standard deviation of the respective population.

Histology. At the end of the experiments, mice were anesthetized with an i.p. overdose of euthanasia solution (Beuthanasia-D, Intervet, Summit, NJ) and intracardially perfused with

phosphate-buffered saline (PBS; 0.01 M, pH 7.2–7.4) followed by 4% paraformaldehyde (PFA) in PBS. Brains were postfixed in PFA overnight at 4°C and then cryoprotected in 30% sucrose in PBS at 4°C. Coronal 30 µm sections were cut on a freezing microtome. Slices separated by either 180 or 90 µm (i.e., either 1 in 6 or 1 in 3 series) were processed for immunohistochemistry after 3 washes in PBS for 10 min each and then transferred to a meshed well where they remained during the entire immunohistochemistry process to prevent tissue damage. For diaminobenzidine (DAB) staining of c-FOS and mCherry-transfected neurons, slices were quenched in 0.3% H_2O_2 in PBS for 30 min before incubation with primary antisera. Slices were incubated in blocking solution (1% Triton X-100 and 5% donkey serum in PBS) at room temperature (RT) for 1 h and then incubated overnight at 4°C in blocking solution containing the primary antibody. After 5 washes in PBS for 5 min each, slices were incubated for 1 h at RT in the secondary antibody and washed 5 times in PBS. For DAB staining, the avidin-biotin-peroxidase system Elite PK-6100 combined with DAB SK-4100 (Vector Laboratories, Burlingame, CA) was used according to the directions. Black c-FOS labeling was obtained by adding nickel chloride to the DAB mix (1.6%).

The primary antisera used (all at 1:2000 dilution) were goat anti-orexin-A (Santa Cruz Biotechnology Cat# sc-8070; RRID:AB_653610) and goat anti-orexin-B (Santa Cruz Biotechnology Cat# sc-8071; RRID:AB_653612), c-FOS rabbit antibody (226003, Synaptic Systems GmbH, Goettingen, Germany; RRID: AB_2231974), chicken anti-GFP (which also recognizes EYFP, Abcam Cat# ab13970; RRID: AB_300798) , rabbit anti-adenosine deaminase (ADA; Cat# AB176, EMD Millipore, Burlington, MA; RRID: AB_2222916) and RFP rabbit antibody

(600-401-379, Rockland, Limerick, PA; RRID: AB_2209751) and rat anti-mCherry antibody (1:1000, Cat# M11217, Thermo Fisher Scientific, Waltham, MA, RRID: AB_2536611).

Secondary fluorescent antisera used were donkey anti-goat (A-11056; RRID: AB_142628) Alexa Fluor 546, donkey anti-rat (Cat# ab150155, Abcam, Cambridge, MA, RRID: N.A.) Alexa Fluor 647, donkey anti-rabbit (A-10042; RRID: AB_2534017) Alexa Fluor 568, donkey anti-rabbit (Cat# A-21206; RRID: AB_2535792) Alexa Fluor 488 and goat anti-chicken (A-11039; RRID: AB_142924) Alexa Fluor 488 (Thermo Fisher Scientific, Waltham, MA). Secondary biotinylated antisera used was donkey anti-rabbit (711-065-152; RRID: AB_2340593, Jackson Immuno Research Laboratories, Inc., West Grove, PA). All secondary antisera were used at a 1:500 dilution. All cell counts were done under double blind conditions.

Results

Transfection of LH cells

With the intention of transfecting only Hcrt neurons, AAV10-TetO-hM3Dq-mCherry (340 nl) was injected bilaterally into the LH of *Orexin-tTA* mice fed with DOX (Fig. 1***A***,***B***). Considerable ectopic expression was observed even though expression of the transgene encoded in this AAV should be dependent on the presence of the tTA and expressed only in the absence of DOX. Because TetO includes a minimal promoter sequence, TetO-linked transgenes can be expressed without tTA if a high enough AAV copy number transfects the cells of interest. To determine whether inhibitory as well as excitatory cells were transfected under these conditions, the same volume of AAV was injected at the same coordinates in *Gad2-IRES-Cre;R26R-EYFP* mice (Taniguchi et al., 2011) in which the glutamate decarboxylase 2 gene (GAD2) is tagged with

yellow fluorescent protein (YFP). Coronal 30 µm sections were cut through the hypothalamus and every 6th section was processed for mCherry and EYFP immunohistochemistry; amplification of EYFP using Alexa Fluor 488 as a secondary antibody was used to label inhibitory neurons in green. The ectopic expression of hM3Dq-mCherry found in *Gad2-IRES-Cre;R26R-EYFP* mice was similar to that observed in *Orexin-tTA* mice. Injections primarily diffused in the ventral and caudal directions and consistently produced neuronal expression of hM3Dq-mCherry in both *Gad2-IRES-Cre;R26R-EYFP* and *Orexin-tTA* mice. Fig. 1***C*** shows that transfected neurons were detected from -0.8 to -2.8 mm relative to bregma. We counted 11,611 transfected neurons from 10 *Gad2-IRES-Cre;R26R-EYFP* mice; 29.9 ± 2.6% of them were GAD2-positive (mean ± SEM) indicating that only a minority of transfected cells were inhibitory. Fig. 1***D*** shows EYFP-labeled inhibitory neurons around the fornix at approximately 1.7 mm from bregma (left), hM3Dq-mCherry expression in the same area (center), and the merged image (right) revealing the rare occurrence of double-labelled (yellow) cells.

To verify that histaminergic (HA) neurons in the tuberomammillary nucleus (TMN) were not transfected by the AAV, we labelled these neurons with rabbit anti-ADA and an anti-rabbit antibody conjugated with Alexa Fluor 488 together with rat-mCherry antibody and anti-rat antibody conjugated with Alexa Fluor 647. We counted unilaterally the number of ADA-labeled cells from a slide corresponding to the TMN at approximately 2.5 mm in the A-P direction from bregma in 8 AAV-transfected *Gad2-IRES-Cre;R26R-EYFP* mice. Out of a total of 177 ADA-labelled cells, only 3 also expressed mCherry, averaging 1.8 ± 0.9% of TMN-HA cells per mouse. Therefore, we conclude that TMN-HA cells were not significantly transfected by the AAV. Fig. 1***E*** illustrates an example of the lack of mCherry on TMN-HA neurons.

LH activation induces several hours of continuous wakefulness

Because the AAV-TetO-hM3Dq-mCherry construct allowed targeting of a broad population of LH cells for experimental manipulation, this AAV was injected in the LH of *Gad2-IRES-Cre;R26R-EYFP* mice (n = 10) that were subsequently implanted for EEG and EMG recordings. To determine whether activation of LH neurons had an effect on sleep/wake, mice were dosed at ZT12 with either clozapine-N-oxide (CNO, 0.5 mg/ml, 3 mg/Kg) or saline (SAL). Fig. 2 shows that *Gad2-IRES-Cre;R26R-EYFP* mice spent close to 100% of the time awake for the first 4 h after CNO administration (***A***) and almost no time in either NREM (***B)*** or REM sleep (***C***) during that period. ANOVA revealed significant interaction of treatment x time on the percentages of time spent in Wake ($F_{(11,88)}$ = 5.2, p < 0.001), NREM ($F_{(11,88)}$ = 5.1, p < 0.001), and REM sleep ($F_{(11,88)}$ = 2.6, p = 0.007) as well as W bout duration (Fig. 2***A'***, $F_{(11,88)}$ = 8.7, p < 0.001, n = 9, two-way repeated measures ANOVA). The hours that were significantly different between treatments are denoted by asterisks (p < 0.05, Bonferroni *post hoc* t-test); significant wake-promoting effects were observed for at least 5 h after CNO injection compared to SAL. Some short NREM sleep bouts were detected during the fourth hour after injection, but the absence of NREM in all subjects for the first several hours precluded statistical comparisons of sleep bout durations (Fig. 2***B'***).

To determine whether a homeostatic response occurred in response to the prolonged wakefulness induced by LH neuron activation, NREM delta power (NRD; defined as spectral power in the 0.5-4 Hz range during NREM sleep) was compared from the first time point after dosing when the hourly average NREM time was at least 20% (which occurred after ZT18-19)

until the end of the recording (Fig. 2***B''***). Despite the prolonged W and reduction of NREM and REM sleep evident in Fig. 2***A-C***, no difference in NRD between CNO and SAL groups or treatment x time interaction was observed for the 6 mice that exhibited NREM bouts during all hours when NREM time was at least 20% ($F_{(1,5)}$ = 3.5 and $F_{(5,25)}$ = 0.9, n.s., n = 6, two-way repeated measures ANOVA).

Because strong wake-promoting effects after LH activation were observed for 5 h after dosing, the distribution of W bout durations during this period was compared between the CNO and SAL groups (Fig. 3***A***). The percentage of time spent in W bouts of 0-1 min and 4-16 min duration was lower after CNO than after SAL injection; in contrast, nearly 80% of the total W time after CNO injection was spent in W bouts > 128 min in duration, which were nonexistent after SAL injection ($p < 0.05$, n = 9; Student's t-test with Bonferroni correction for multiple comparisons). Nonetheless, comparison of the distribution of W bout durations between CNO and SAL treatments did not quite reach statistical significance (p = 0.051, n = 83 and 274 bouts for CNO and SAL treatments, respectively; two-sample Kolmogorov-Smirnov goodness-of-fit hypothesis test).

As a control for CNO injection, a cohort of naïve C57BL/6J mice (n = 8) were instrumented for EEG/EMG recordings and, after recovery from surgery and acclimation to the experiment, received either CNO (3 mg/Kg, i.p.) or SAL during the inactive phase at ZT5 when any increase in W time should be readily evident. Fig. 3***B*** presents the hourly percentage of W time after dosing for both treatments. No significant difference was found in the percentage of time in any state, bout duration or any frequency band in the power spectrum between the two treatment conditions.

Because *Gad2-IRES-Cre;R26R-EYFP* mice remained continuously awake for several hours after CNO injection, we analyzed the EEG power spectrum and no grossly abnormal patterns in EEG activity were detected (Fig 3***C-E***). However, a pronounced peak occurred in the 8-10 Hz range (high theta, Hθ) during W, a higher frequency than the θ peak observed during REM sleep which is centered around 7 Hz. Fig. 3***C*** shows a trend towards elevated Hθ power during W (HθWP) for 5 h after dosing. Statistical analysis confirmed a significant treatment x time interaction ($F_{(11,88)} = 4.2$, $p < 0.001$, $n = 9$, two-way repeated measures ANOVA), although *post hoc* analysis determined that ZT14-15 was the only hour during which HθWP was significantly elevated (Fig. 3***C***). The normalized mean power spectrum between ZT13 and ZT15 during W was slightly higher after CNO dosage for most frequencies (Fig. 3***D***). In order to quantify the differences in normalized power between conditions, we grouped the frequencies into the bands described in the Methods: δ, Lθ, Hθ, Lγ, Hγ and Vhγ (Fig. 3***E***). A significant interaction of treatment x power band was observed ($F_{(5,40)} = 4.5$, $p = 0.002$, $n = 9$, two-way repeated measures ANOVA). *Post hoc* analysis showed significantly elevated power during ZT13-15 for Hθ, Hγ and Vhγ, which were 27%, 28% and 21% greater, respectively, after CNO injection.

LH activation induces a physiological increase in locomotor activity

To determine whether LH activation by CNO injection induced abnormal behavior, the activity of 9 *Gad2-IRES-Cre;R26R-EYFP* mice was recorded in their home cage by infrared video with concurrent EEG/EMG recordings for 2 h after dosing. Using the positions extracted from the video, we calculated the instantaneous speed of locomotion and then an average speed per 4-s epoch for each recording. When W epochs were compared, the overall range of values for

mean locomotor velocity per epoch (0-16 cm/s) was similar for both treatments. However, the probability distribution of velocities from all mice under the two treatments were significantly different ($p < 10^{-308}$, n = 14,067 and 11,016 epochs of W for CNO and SAL treatments respectively, two-sample Kolmogorov-Smirnov goodness-of-fit hypothesis test). CNO-injected mice showed a trend towards spending more time at velocities above 2 cm/s, while SAL-injected mice spent more time at speeds below 2 cm/s (Fig. 3***F***). The Mean W speed after SAL injection was 0.9 ± 0.2 cm/s and 1.7 ± 0.3 cm/s after CNO (p = 0.046, n = 9, t-test). Thus, LH activation tends to increase activity by changing the proportion of slow vs. fast speeds rather than by causing the mice to move at an abnormal speed in its home cage.

From hippocampal electrode recordings, it is well established that rodents increase θ power during exploration and active behavior (Vanderwolf, 1969; Shin et al., 2001; Hinman et al., 2011; Bender et al., 2015). We observed a strong correlation between HθWP and movement velocity when measuring cortical EEG. Fig. 3***G*** shows the temporal dynamics of mean locomotor speed per epoch (black trace) and scale-adjusted HθWP (green trace) for a mouse injected with CNO. The mean Pearson correlation between speed and HθWP after SAL and CNO injection were 0.44 ± 0.04 and 0.36 ± 0.07, respectively, reflecting a highly significant correlation in both cases (mean $p < 10^{-39}$). No seizure-like activity or any sign of abnormal behavior was observed in CNO-injected animals, except for an increase in active wakefulness that was characterized by the same physiological parameters of locomotor speed and EEG power that occurred during active periods after SAL injection.

CNO-induced wakefulness is independent of Hcrt signaling

The nonspecific LH neuron transfection that resulted in the potent W-promoting effects after CNO injection at ZT12 (Fig. 2***A*** and ***A'***) might be due to activation of Hcrt neurons. As a first step to evaluate this possibility, we administered the dual orexin receptor antagonist almorexant (ALM) to *Gad2-IRES-Cre;R26R-EYFP* mice at a high dose (200 mg/Kg, i.p.) and at a time of day (ZT12) at which we had previously shown ALM to be sleep-inducing in other rodent strains (Morairty et al., 2012; Black et al., 2013). As in our previous studies, ALM increased the time spent in NREM sleep and decreased both the W time percentage and W bout duration, in this case, for more than 5 h relative to VEH (data not shown). Thus, ALM effects on sleep architecture were the inverse of those observed in response to LH activation and had a similar time course.

To further test whether Hcrt signaling was required for the observed increase in W time after LH activation and whether time-of-day affects CNO-induced W promotion, we performed a dual-dosing study in which mice were treated with either VEH or ALM (200 mg/Kg, i.p.) during the inactive period at ZT4 and, 1 h later, injected with either CNO (3 mg/Kg, i.p.) or SAL while EEG and EMG were continuously recorded from ZT3 to ZT12. Fig. 4 shows the percentage of time spent in each behavioral state (upper panels) and the mean bout duration of each state (lower panels), revealing a strong wake-promoting effect of CNO injection even in the presence of Hcrt receptor blockade by ALM (blue line). When all time points after dosing (ZT5-ZT12) were analyzed, significant treatment x time interactions were identified for the percentages of W ($F_{(18,162)}$ = 31.1, p < 0.001, Fig. 4***A***), NREM ($F_{(18,162)}$ = 32.4, p < 0.001, Fig. 4***B***) and REM sleep

($F_{(18,162)}$ = 5.4, p < 0.001, Fig 4***C***; n = 10, two-way repeated measures ANOVA). There were no differences between the ALM-CNO and VEH-CNO treatments in the percentage of any state. However, the mean W bout duration, for which there was a significant treatment x time interaction ($F_{(18,162)}$ = 17.4, p < 0.001), was significantly shorter in the ALM-CNO compared to the VEH-CNO treatment. These results indicate that, despite the strong wake-promoting effect of LH neuron activation produced by CNO injection, ALM reduced the mean W bout duration (Fig. 4***A'***) due to occasional NREM episodes that interrupted sustained W bouts but were too brief (< 12 s) to constitute a NREM bout. Due to the absence of sleep bouts from most mice after CNO injection, no statistical analysis was performed on sleep bout durations (Fig. 4***B'***,***C'***).

In contrast to the active period (Fig. 3***D***), LH activation during the inactive period induced a large increase in the EEG power spectrum, especially in the Hθ and > 50 Hz ranges (Fig. 5***A***). When the normalized power values during W were analyzed by conventional spectral bands, a significant treatment x power band interaction was found ($F_{(15,135)}$ = 16.3, p < 0.001, n = 10, two-way repeated measures ANOVA), as depicted in Fig. 5***B*** where the symbols above the bars denote significant differences between pairs of conditions according to the legend in Fig. 5***E***. The normalized power for the VEH-CNO treatment (magenta) was significantly greater than that observed after VEH-SAL treatment (black) for the Hθ, Lγ, Hγ and Vhγ bands by 120%, 42%, 107% and 76%, respectively.

The distribution of W bout durations (Fig. 5***C***) differed for most treatments during the first 5 h after dosing (ZT5-10). Pairwise comparison of the Wake Bout Duration distribution between treatments using the two-sample Kolmogorov-Smirnov goodness-of-fit hypothesis test with Bonferroni correction showed that all but the VEH-SAL vs. ALM-SAL comparison (p = 0.51)

were significantly different ($p < 0.0073$, number of bouts = 636, 755, 294 and 592 for ALM-CNO, ALM-SAL, VEH-CNO and VEH-SAL, respectively). Fig 5***C*** shows that dosing with ALM-SAL (green), not surprisingly, suppressed long W bouts; most of the time awake was spent in short W bouts. Conversely, most of the W time in the VEH-CNO treatment (magenta) was spent in long W bouts and the W bout distribution was shifted to the right. The W bout distribution for the ALM-CNO (blue) and VEH-SAL (black) treatments were intermediate between the other two treatments.

A strong treatment x time interaction was observed for the HθWP after dosing ($F_{12,108}$ = 5.3, $p < 0.001$, $n = 10$, two-way repeated measures ANOVA). *Post hoc* analysis revealed that the VEH-CNO treatment was significantly different than the other three treatments during several hours, as depicted by the symbols above the respective ZT points in Fig. 5***D***. VEH-CNO dosing (magenta) enhanced HθWP but this effect was suppressed when combined with ALM (ALM-CNO; blue), which differed from the ALM-SAL treatment (green) at one time point only; there was no difference between treatments in the absence of CNO.

To determine the homeostatic response to CNO-induced W during the inactive period, we compared NRD from the first time point after dosing when the average NREM time was at least 20% within an hour (which occurred after ZT8). A main effect of drug treatment on NRD was found ($F_{(3,24)} = 3.7$, $p = 0.024$, $n = 9$, two-way repeated measures ANOVA) without a treatment x time interaction ($F_{(9,72)} = 0.74$, n.s.). Fig. 5***E*** shows that NRD after VEH-CNO (magenta) was higher than after ALM-CNO (blue), despite similar amounts of prior W after both treatments (Fig. 4***A***).

CNO-induced arousal is likely due to activation of a novel LH wake-promoting neuronal population

The currently known wake-promoting populations in the LH are the Hcrt neurons and two groups of GABAergic neurons (Herrera et al., 2016; Venner et al., 2016). To determine whether these wake-promoting cells were involved in the strong wake promotion described above, at least one week after the last dosing experiment, *Gad2-IRES-Cre;R26R-EYFP* mice received either CNO or SAL at ZT3 followed by 90 min of sleep deprivation (SD) by cage tapping or movements of the nesting material in their home cages and were then perfused transcardially with 4% PFA. SD was necessary because CNO-treated mice spent all 90 min awake while mice injected with SAL at ZT3 sleep for a large proportion of the 90 min after injection, which would result in differences in c-FOS expression that would be due to the difference in behavioral state rather than to activation by CNO. Since mice spend most of the time asleep between ZT0-ZT3 and thereby discharge homeostatic sleep drive, SD can be performed for 90 min after ZT3 with minimal intervention. Consequently, SD for 90 min beginning at ZT3 allowed us to compare c-FOS expression during wakefulness with or without hM3Dq activation of LH neurons.

Brain tissue was sectioned in 30 μm coronal slices, divided into 6 series and processed for expression of the immediate early gene c-FOS as an indicator of neuronal activity and for expression of Hcrt, EYFP and mCherry. To determine whether hM3Dq was expressed in Hcrt neurons, we performed double immunohistochemistry on 4 *Gad2-IRES-Cre;R26R-EYFP* mice by co-incubation with anti-Hcrt1/orexin-A and anti-Hcrt2/orexin-B antisera followed by an mCherry (rabbit anti-RFP) antibody which reported hM3Dq expression. Of the 627 ± 21 Hcrt

456 cells found on average in each mouse, 14 ± 2% also expressed mCherry as depicted in Fig. 6***A*** in
457 which only 6 Hcrt neurons are also labelled by mCherry (white arrows).
458 Together with the results shown in Fig. 1, the data above can be used to estimate the
459 approximate percentage of transfected cells that are Hcrt neurons. Because we counted on
460 average 1,161 hM3Dq-transfected neurons in each tissue series, we can expect to find
461 approximately 7,000 transfected cells in each *Gad2-IRES-Cre;R26R*-EYFP mouse. Because AAV
462 expression occurred in approximately 14% of Hcrt cells and, assuming there are about 4,000
463 Hcrt neurons in a mouse (McGregor et al., 2017), we estimate that about 560 Hcrt neurons
464 were transfected in each mouse which corresponds to less than 8% of the total number of
465 transfected neurons.
466 Although Hcrt cells were not directly activated by hM3Dq and ALM dosing did not
467 decrease the wake-promoting effects of CNO, it is still possible that Hcrt cells were indirectly
468 activated and promoted arousal via glutamatergic excitation of its targets. To determine
469 whether CNO causes a robust increase in c-FOS expression in Hcrt cells, we counted the number
470 of Hcrt neurons expressing c-FOS after either CNO or SAL injection to assess whether they were
471 indirectly activated as a downstream target. We counted on average 353 ± 70 Hcrt neurons per
472 mouse in the CNO group (1,766 Hcrt neurons in total) in which 68.8 ± 5.5% were FOS^+,
473 compared to 429 ± 38 Hcrt neurons/mouse in the SAL group (2,143 Hcrt neurons in total) in
474 which 54.8 ± 5.7% were FOS^+ ($p = 0.119$, $n = 5$, *t*-test). Thus, CNO injection did not cause a
475 significant increase in c-FOS expression in Hcrt neurons during W in *Gad2-IRES-Cre;R26R-EYFP*
476 mice. Fig. 6***B*** shows the Hcrt field and the negative image of c-FOS staining using DAB for a
477 mouse injected with CNO 90 min before perfusion. Arrows indicate Hcrt neurons that did not

express c-FOS and show that, despite the strong wake-promoting effects of CNO, a large percentage of Hcrt neurons was not activated.

Although the majority of transfected neurons by the AAV-TetO-hM3Dq-mCherry construct were not inhibitory, it is possible that CNO injection may activate either directly, or indirectly via downstream activation, one or both of the wake-promoting inhibitory neuronal populations recently described in the LH. In this case, the CNO-activated LH cells might project to and inhibit thalamic reticular nucleus (nRT) neurons (Herrera et al., 2016) and/or wake-promoting neurons located around and lateral to the fornix that are thought to project to and inhibit the ventrolateral preoptic area (VLPO) (Venner et al., 2016). We reasoned that, if the mechanism of arousal observed in this study was due to activation of either of these pathways, there should be evidence of either strong activation of inhibitory neurons around the fornix or a suppression of activity in the nRT after activation of hM3Dq-transfected neurons. Fig. 6***C*** illustrates that CNO induced robust activation of hM3Dq-expressing neurons in the perifornical area, with c-FOS in black and mCherry (the hM3Dq reporter) in brown after SAL (upper panel) vs. CNO (lower panel) injection.

To determine whether the pathways mentioned above were recruited after CNO injection, we performed YFP/c-FOS double immunohistochemistry in the same cohort of mice studied above. The number of double-labeled neurons in both hemispheres were counted from two slices from each of 10 *Gad2-IRES-Cre;R26R-EYFP* mice, sectioned around -1.7 mm from bregma. A ~100 μm perimeter plus an area at an approximately 45° angle from this perimeter laterally to the edge of the hypothalamus in the dorsal and ventral directions was delineated for cell counts. Fig. 6***D*** illustrates that this delineated area (white dotted line)

500 includes both the perifornical area and the lateral hypothalamus. In this panel, inhibitory
501 neurons are in green and c-FOS expression in black from mice injected either with SAL (upper
502 panel) or CNO (lower panel) showing that few $Gad2^+$ neurons exhibited c-FOS expression. The
503 average number of double-labelled inhibitory cells in this hypothalamic area did not differ
504 between groups (48.4 ± 13 $c\text{-}FOS^+$ cells per mouse after SAL injection, 242 double-labelled cells
505 in total vs. 75 ± 24.4 $c\text{-}FOS^+$ cells after CNO injection, 375 cells in total; $p = 0.36$, *t*-test, $n = 5$). In
506 both conditions, the majority of inhibitory neurons did not express c-FOS; consequently, we did
507 not calculate the percentage of double-labelled cells among all inhibitory neurons.

508 Similarly, Fig. 6***E*** shows the expression of c-FOS in the nRT after systemic injection of
509 either SAL (upper panel) or CNO (lower panel). c-FOS-labelled inhibitory cells were identified
510 bilaterally in coronal slices of the nRT region at 1.4-1.8 mm from bregma in one slide per
511 mouse. In both treatments, c-FOS expression was very rare; thus, the percentages were not
512 calculated and only the total number of double-labelled cells was counted (53.4 ± 9.8 cells per
513 mouse after SAL injection, 267 double-labelled cells in total vs. 55 ± 8 cells per mouse after CNO
514 injection, 275 double-labelled cells in total; $p = 0.9$, *t*-test, $n = 5$).

515 The volume of AAV injected (340 nl) was intended to ensure transfection of the entire
516 LH; the injections spread ventrally and dorsally up to the mammillary nucleus. Recently, it was
517 found that chemogenetic activation of glutamatergic neurons in the supramammillary nucleus
518 (SuM) promote wake without increasing locomotion, yet all EEG parameters indicative of active
519 wake are increased (Pedersen et al., 2017). To determine whether CNO treatment caused a
520 significant increase in c-FOS expression in SuM neurons, we also counted c-FOS expression in
521 this region in 4 mice treated with SAL (a total of 2,732 cells expressing c-FOS, 683±64

cells/mouse) and 5 mice treated with CNO (3,421 cells in total, 684±61 cells/mouse) but found no evidence of a significant difference in c-FOS expression in the SuM between treatments (p = 0.99, t-test, n = 4 & 5). Fig. 7 illustrates these results, showing similar or even greater c-FOS expression in a mouse treated with saline (Fig. 7***A***) compared to a mouse treated with CNO (Fig. 7***B***). Although some hM3Dq transfection was observed in this region, it was mostly on the edge of the lateral mammillary nucleus and not in the SuM itself (Fig. 7***C***).

Dissection of Hcrt vs non-Hcrt arousal pathways

Fig. 4***A*** demonstrated that LH activation can evoke potent arousal during the inactive phase even in the presence of Hcrt receptor blockade and Figs. 6***A*** and 6***B*** show that Hcrt neurons are neither directly nor indirectly involved in the potent wake promotion observed. However, this unknown LH wake-promoting population might have a downstream mechanism for wake promotion similar to that of the Hcrt neurons, i.e., these neurons may project to and excite known wake-promoting targets such as the TMN and LC. On the other hand, the observed wake-promoting action might be exerted via a different, parallel wake-promoting pathway yet to be described. We hypothesized that, if the wake-promoting pathway activated here overlaps with the Hcrt pathway, co-activation of both neuronal populations should trigger only minor differences when compared to activation of non-Hcrt neurons alone. On the other hand, if it is possible to further increase W after co-activation of Hcrt neurons, that would imply that Hcrt and non-Hcrt pathways are independent of each other.

To distinguish between these possibilities, we took advantage of the tTA dependence of the AAV-TetO-hM3Dq-mCherry construct. When neurons that express tTA are exposed to this

AAV, a large percentage is expected to become transfected in addition to the ectopic expression depicted in Fig. 1. Therefore, by adding or removing DOX from the mouse diet, the expression of hM3Dq in the tTA population can be manipulated. Consequently, we injected AAV-TetO-hM3Dq-mCherry bilaterally into the LH of *Orexin-tTA* mice that expressed tTA only in the Hcrt neurons. When *Orexin-tTA* mice were fed with DOX chow, ectopic expression occurred to a similar degree to that observed in *Gad2-IRES-Cre;R26R-EYFP* mice (Fig. 1***B***) but expression of hM3Dq-mCherry within Hcrt neurons was suppressed, as depicted in Fig. 8***A*** where little overlap exists between the Hcrt neurons and hM3Dq-mCherry-expressing cells (denoted by 8 white arrows). When DOX was removed from the chow for at least 3 weeks, in addition to the ectopic expression, transfected Hcrt neurons also expressed hM3Dq and could therefore be activated by CNO. Fig. 8***B*** shows that, in the absence of DOX, the hM3Dq-mCherry transgene is strongly expressed in the Hcrt neurons, denoted by 32 white arrows. In a series of coronal sections separated by 120 µm in 3 mice that had been fed with DOX chow for at least 4 weeks, there were 447 ± 17 Hcrt neurons per mouse (1,340 neurons in total) of which only 18.0 ± 5.0% of Hcrt neurons expressed hM3Dq-mCherry. In contrast, in 3 mice that were fed with normal chow, there were 315 ± 112 Hcrt neurons per mouse (946 neurons in total) of which 62.2 ± 13.2% of Hcrt neurons expressed hM3Dq-mCherry. Thus, the absence of DOX in the diet enhanced expression of hM3Dq-mCherry in Hcrt neurons by more than 3-fold.

To study the effect of LH activation with or without concurrent Hcrt activation, we performed the same dosing study as in Fig. 4, but we used *Orexin-tTA* mice fed with either normal chow or DOX chow. Although we injected AAV-TetO-hM3Dq-mCherry in 21 *Orexin-tTA* mice, 7 mice did not show high levels of ectopic expression nor a significant increase in W

during the first 2 h after CNO injection and therefore were excluded from analysis. From the 14 remaining mice, 1 was studied only under the DOX(+) condition, 3 were studied only in absence of DOX, and the remaining 10 mice were studied under both the DOX(+) and DOX(-) conditions. In these 10 mice, the second dosing study occurred at least 3 weeks after removal of DOX from the chow. As in the study illustrated in Fig. 4, we injected either ALM or VEH at ZT4 and either CNO or SAL at ZT5 while continuously measuring EEG/EMG from ZT4 to ZT11.

In the DOX(+) condition when only a small percentage of Hcrt cells expressed hM3Dq, both VEH-CNO and ALM-CNO treatments evoked a strong increase in W time in a similar manner to that observed in *Gad2-IRES-Cre;R26R-EYFP* mice (Fig. 4***A***) and a strong treatment x time interaction occurred ($F_{(15,150)} = 8.5$, $p < 0.001$, $n = 11$, 2-way repeated measures ANOVA) as depicted in Fig. 8***C***. VEH-CNO (magenta) and ALM-CNO (blue) treatments did not differ from each other but they were significantly different from VEH-SAL (black) and ALM-SAL (green) for most of the time points. In the DOX(-) condition in which about 62% of Hcrt cells were transfected, a similar result was observed, i.e., strong wake-promoting effects after CNO dosing regardless of the presence of ALM and a significant treatment x time interaction ($F_{(15,180)} = 5.6$, $p < 0.001$, 2-way repeated measures ANOVA). A trend towards a stronger and longer-lasting W promotion was evident for the VEH-CNO (magenta) compared to ALM-CNO treatment (blue; Fig. 8***D***) but, since there was also a large amount of W in presence of ALM, the difference was not significant, likely due to a ceiling effect.

To further analyze the effect of dietary DOX and the difference in W promotion between the ALM-CNO and VEH-CNO treatments, we calculated the cumulative increase in W time for VEH-CNO and ALM-CNO treatments relative to the VEH-SAL treatment in both the DOX(+) (Fig.

588 8***E***) and DOX(-) (Fig. 8***F***) experimental groups after dosing. Whereas there was no significant
589 difference between these treatments in the DOX(+) condition (p = 0.29, n = 11, t-test; Fig. 8***E***),
590 the concurrent activation of Hcrt neurons and other LH cells in the DOX(-) condition resulted in
591 a significant difference in the W time increase in the VEH-CNO treatment relative to the ALM-
592 CNO treatment (p = 0.029, n = 13, t-test; Fig. 8***F***). CNO activation of Hcrt neurons might cause
593 glutamate release by Hcrt neurons which could contribute to the W increase after the ALM-
594 CNO combination. Comparing the blue bars in Figs. 8***E*** and 8***F***, DOX(-) mice exhibited 26.2 ± 14.1
595 min more W time than DOX(+) mice after ALM-CNO treatment but this difference was not
596 significant (n.s., n_1 = 11, n_2 = 13, two-sample t-test), suggesting a minor role for glutamatergic
597 excitation in the observed increase in W time. A two-way unbalanced ANOVA revealed a
598 significant effect of drug treatment ($F_{(1,1)}$ = 5.47, n_1 = 11, n_2 = 13, p = 0.024) and type of chow
599 ($F_{(1,1)}$ = 5.11, n_1 = 11, n_2 = 13, p = 0.029), but no interaction between drug and type of chow
600 ($F_{(1,44)}$ = 0.38, n.s., two-way unbalanced ANOVA, Table 2).
601

602 **Discussion**

603 Although the Hcrt cells are a small subset of the entire LH population, they are the only
604 excitatory wake-promoting neurons currently known in this brain region and are thought to
605 stabilize wakefulness via excitation of wake-promoting centers like the TMN, LC and BF. Here,
606 we have shown that chemogenetic excitation of LH neurons evokes sustained arousal in an
607 Hcrt-independent manner. The existing literature, which has documented lethargy after
608 suppression of neuronal activity in this area, supports the concept that LH neurons are essential
609 to sustain wakefulness. The current results demonstrate that LH neuron activation promotes

arousal without producing aberrant behavior or EEG anomalies, indicating that non-Hcrt neurons in LH could be part of the endogenous sleep-wake regulatory system. The fact that concurrent excitation of Hcrt neurons produced even a greater level of arousal (Fig. 8***D,F***) suggests that this putative novel wake-promoting system has a parallel, Hcrt-independent mechanism of action that could promote wakefulness via different downstream targets.

LH neuron activation produces physiological wakefulness without excessive hyperactivity

LH neuron activation during the active phase caused mice to remain awake almost continuously for 4 h (Fig. 2***A***), 1h longer than during the inactive phase (Fig. 4***A***), suggesting a circadian influence on W promotion. The change in sleep architecture underlying this increased wakefulness involved a shift toward longer duration W bouts (Figs. 3***A,*** 5***C***) rather than an increased number of W bouts.

The EEG during these sustained W bouts resembled the W EEG during the active phase, although the spectral power in the Hθ, Hγ and Vhγ bands increased by 20-30% (Fig. 3***D***,***E***). During the inactive phase, LH activation increased spectral power in the Hθ band by 120% (Fig. 5***A,B***) which was directly correlated with the speed of locomotion (Fig. 3***G***) and large increases in spectral power also occurred in the gamma range. It was shown recently that Hcrt as well as GABAergic neurons in LH directly regulate locomotor behavior (Kosse et al., 2017; Perez-Leighton et al., 2017; Qualls-Creekmore et al., 2017) and that hippocampal neurons that give rise to the θ rhythm observed in the EEG during locomotion can activate inhibitory neurons in the lateral septum that, in turn, inhibit LH neurons and thereby reduce locomotor speed (Bender et al., 2015). Therefore, activation of LH neurons might activate circuits that regulate

632 locomotor activity itself and not necessarily arousal. Strong activation of these circuits should
633 evoke non-physiological behaviors due to the potent activation observed after CNO treatment
634 in hM3Dq-transfected cells (Fig. 6***C***). Nevertheless, despite the large increase in HθWP after
635 VEH-CNO treatment (Fig. 5), the maximum absolute values (between 0.5 and 0.6 μV^2) were
636 similar to those observed during the active phase suggesting that mice were as active after CNO
637 injection at ZT5 as during active wake after ZT12 and, therefore, that the changes in locomotor
638 activity are due to changes in behavioral state rather than to manipulation of neuronal circuits
639 that regulate locomotion. The range of velocities observed in mice injected with CNO was
640 similar to those observed after SAL injection; however, CNO-injected mice spent more time
641 moving at higher speeds (Fig. 3***F***). Together, these findings suggest that LH activation after
642 transfection with AAV-TetO-hM3Dq produces physiologically normal wakefulness.
643 To be part of the physiological regulation of sleep and wake, wake-promoting neurons
644 should not cause aberrant EEG patterns or pathological behavior, should be active either during
645 or at the onset of wake, and suppression of their activity should cause a decrease in arousal.
646 Here, we have shown that activation of an unknown LH population can indeed cause active
647 wake without aberrant behavior nor EEG anomalies, indicating that these LH cells could be
648 considered part of the physiological regulation of arousal. Future work will determine whether
649 they are necessary and sufficient to sustain wake.
650
651 **Is the observed arousal caused by a novel hypothalamic wake-promoting neuronal**
652 **population?**

Histaminergic neurons in the TMN have been shown to be wake-promoting, yet immunohistochemistry revealed that this cell group was not transfected by our AAV (Fig. 1***E***) despite the presence of some transfected cells in this region of the hypothalamus. Two wake-promoting GABAergic neuronal populations have recently been described in the LH. Inhibitory nRT-projecting LH neurons have been shown to induce wakefulness upon acute stimulation during NREM but not during REM sleep (Herrera et al., 2016), yet we showed that the amount of c-FOS expression in nRT was very low and there was no difference in c-FOS expression whether mice received CNO or SAL while being kept awake (Fig. 6***E***). Although the absence of FOS expression does not necessarily mean that neurons were inactive, it is unlikely that a further reduction in nRT activity mediated by LH GABAergic input after CNO dosing would trigger the robust wake-promoting response shown here. Similarly, VLPO-projecting inhibitory neurons located in the perifornical area have been proposed to promote wake by inhibiting the sleep-active inhibitory neurons in VLPO (Venner et al., 2016). Because only a minority of inhibitory neurons in the perifornical area expressed c-FOS and the number of c-FOS^{+} cells did not change after CNO vs. SAL injection (Fig. 6***D***), it is unlikely that the increase in W time and locomotor activity was caused by only sparse excitation of VLPO-projecting inhibitory neurons. Because about 30% of transfected neurons in LH were GABAergic, it is possible that the CNO-activated LH population included some of these novel wake-promoting cell groups. Recently, glutamatergic wake-promoting neurons were found in the supramammillary (SuM) region (Pedersen et. al., 2017). Although we observed some transfected cells in this region, transfection was sparse and mostly lateral and ventral to the SuM (Fig. 7***C***). Since SuM neurons expressed significant c-FOS during wake regardless of treatment, the marginal increase on the

edges, which seemed to cause an increase in c-FOS expression in the lateral mammillary nucleus, did not affect the overall expression of c-FOS in SuM. More importantly, mice were described in that study as often stationary after CNO treatment, there was no correlation between increase in Hθ activity and locomotion, and the EMG was similar to control levels during the inactive phase. These results are the opposite of what we obtained (see, for example, Fig. 3 ***E***,***F***); thus, although some of these wake-promoting cells could have been activated, it is unlikely they are the main source of the observed arousal. Although more experiments will be required to demonstrate that LH wake-promoting neurons activated in the present study are a different population than currently known wake-promoting populations, our evidence points in that direction.

Concurrent activation of LH wake-promoting neurons and Hcrt neurons enhances arousal

Because thousands of neurons were transfected in *Gad2-IRES-Cre;R26R-EYFP* mice which lack tTA (Fig. 1***C,D***), the AAV-TetO virus did not restrict expression to only tTA neurons. However, this partial tTA dependence enabled an interesting strategy to compare the physiological effects of LH activation when different proportions of Hcrt neurons expressed the hM3Dq receptor. In mice maintained on a DOX(+) diet, 18% of Hcrt cells expressed hM3Dq-mCherry as well as a much larger number of non-Hcrt cells. There was no difference in the amount of wakefulness produced by CNO injection whether these mice received SAL or ALM pretreatment. In contrast, 62% of Hcrt neurons in DOX(-) mice expressed hM3Dq-mCherry and, in these mice, ALM pretreatment attenuated the increase in W time produced by CNO injection with respect to the VEH-SAL treatment. Thus, concurrent Hcrt and non-specific LH neuron

activation produced more robust arousal as shown by the significant effect of Dox chow shown in Table 2. The lack of a significant interaction between chow and treatment can be attributed to ceiling effects.

Hcrt neurons are also glutamatergic although, to our knowledge, there is no direct *in vivo* evidence of a role for glutamate release by the Hcrt neurons in the regulation of sleep and wake. Because ALM blocks the excitation mediated by Hcrt peptides but not glutamatergic excitation, comparison of the increase in W time under the ALM-CNO treatment between the DOX(-) and DOX(+) conditions might reveal the magnitude of glutamatergic-mediated arousal. We suggest that glutamatergic excitation mediated by Hcrt neurons has a secondary role in wake promotion because the difference in W amount between these two conditions (Fig. 8***E*** vs. 8***F,*** blue bars) was not significant.

Potential therapeutic target for sleep disorders

During the inactive phase, the time-weighted frequency histograms for the ALM-SAL treatment shifted toward shorter W bout durations (Fig. 5***C***), reflecting an inability to sustain prolonged W bouts after Hcrt blockade that is reminiscent of the symptomatology of narcoleptic patients. In the ALM-CNO treatment, activation of the parallel LH arousal pathway induced prolonged W bouts despite blockade of Hcrt signaling which demonstrates that it is possible to achieve consolidated W in the absence of Hcrt signaling. Activation of this novel arousal pathway may also provide treatment for hypersomnia. Conversely, based on lesion and inactivation experiments performed by others, we hypothesize that suppression of the activity of this LH pathway promotes sleep, suggesting a potential treatment for insomnia. Future work will focus

719 on the molecular neuroanatomical identification of these LH wake-promoting neurons, their
720 activation and inhibition, as well as identification of their afferent inputs, efferent targets and
721 the neurotransmitters involved.
722

Figure Legends

Figure 1. Expression of hM3Dq in the LH. ***A***. Schematic of the AAV utilized. ***B***. AAV-injected *Orexin-tTA* mice exhibited widespread neuronal expression of hM3Dq-mCherry despite the presence of DOX in the chow. ***C***. Despite the absence of tTA, *Gad2-IRES-Cre;R26R-EYFP* mice injected with AAV-TetO-hM3Dq-mCherry exhibited a pattern of hM3Dq-mCherry expression that was similar to DOX-fed *Orexin-tTA* mice. Scale bar in ***B*** and ***C*** denotes 250 µm. Numbers in the upper left in ***C*** denote approximate AP distance from bregma (mm). ***D.*** Photomicrographs showing GAD2-EYFP$^+$ neurons lateral to the fornix (Fx, left), hM3Dq-mCherry transfected neurons (center) and double-labeled neurons in yellow after merging both images (right). Scale bar denotes 100 µm. M and L denote medial and lateral. ***E***. Photomicrographs showing ADA$^+$ neurons in TMN (left), hM3Dq-mCherry transfected neurons (center) and merged image (right) showing the absence of double-labeled neurons. Scale bar denotes 50 µm.

Figure 2. LH activation induces continuous wakefulness for at least 4 h. Hourly percentage of time spent in W (***A***), NREM (***B***) and REM sleep (***C***) and hourly bout duration for W (***A'***) and NREM (***B'***) after injection of either CNO (red) or SAL (black). Asterisks denote significant difference between CNO and SAL treatment for the respective hour when a significant treatment x time interaction was found ($p \leq 0.047$, $n = 9$; 2-way repeated measures ANOVA, Bonferroni *post hoc t*-test). ***B''***. No significant change in NREM delta power was observed after the prolonged W induced by CNO injection (*n.s.*, $n = 6$, 2-way repeated measures ANOVA). Arrow at bottom left of abscissa indicates time of dosing at ZT12.

745

746 **Figure 3**. Characterization of CNO-induced wakefulness. ***A***. Time-weighted frequency
747 histograms showing the proportion of wake bouts of each duration (WBD) relative to the total
748 amount of wakefulness from ZT12 to ZT17 after CNO or SAL treatment in *Gad2-IRES-Cre;R26R-*
749 *EYFP* mice. Asterisks denote significant differences ($p < 0.04$, $n = 9$, *t*-test with Bonferroni
750 correction for multiple comparisons). ***B***. Hourly percentage of time spent in W for naïve WT
751 mice injected with CNO or SAL during the inactive phase. ***C.*** HθWP in the dark period after CNO
752 or SAL dosing of *Gad2-IRES-Cre;R26R-EYFP* mice at ZT12. Asterisk denotes a significant
753 difference for the respective hour when a significant treatment x time interaction was found (p
754 = 0.046, $n = 9$; 2-way repeated measures ANOVA, Bonferroni *post hoc t*-test). ***D***. Normalized
755 EEG power spectrum during W averaged from ZT13 to ZT15 after dosing of *Gad2-IRES-*
756 *Cre;R26R-EYFP* mice with CNO (red) or SAL (black) at ZT12. ***E***. Mean power for EEG spectral
757 bands of *Gad2-IRES-Cre;R26R-EYFP* mice after dosing with either CNO or saline, normalized by
758 baseline. Asterisk denotes a significant difference for the respective band when ANOVA
759 revealed a significant treatment x power band ($p = 0.002$, $n = 9$; 2-way repeated measures
760 ANOVA, Bonferroni *post hoc t*-test). ***F***. Percentage of time mice spent moving at different
761 speeds from ZT12 to ZT14 during W. ***G***. Example of simultaneous recordings of mean speed per
762 epoch (black trace) and scale-adjusted HθWP (green trace).

763 **Figure 4**. Hcrt signaling is not required for LH activation-induced arousal. Upper panels show
764 hourly percentage of time spent in W (***A***), NREM (***B)*** and REM sleep (***C***) and lower panels (***A'- C'***)
765 show corresponding mean hourly bout duration for each state after injection of either VEH or
766 ALM during the inactive phase at ZT4 followed by either SAL or CNO at ZT5. Arrows at the

767 bottom left of the abscissa in ***A'***, ***B'*** and ***C'*** indicate the times of dosing. Symbols above each
768 time point denote significant hourly differences between the indicated treatments according to
769 the legends in panels **A** and **A'** when a significant treatment x time interaction was found ($p <$
770 0.001, $n = 10$, 2-way repeated measures ANOVA, Bonferroni *post hoc t*-test).

771 **Figure 5**. LH activation at ZT5 increases spectral power in the Hθ and gamma bands of the EEG
772 during W. ***A***. Normalized EEG power spectrum during W averaged from ZT6 to ZT8 for the
773 different experimental treatments. ***B***. Mean power in the spectral bands of the EEG after
774 treatment, normalized to baseline. ***C***. Time-weighted frequency histograms showing the
775 proportion of wake bouts of each duration (WBD) relative to the total amount of wakefulness
776 from ZT5 to ZT10 for the different experimental treatments. ***D***. HθWP for the different
777 experimental treatments. ***E***. NREM delta power for all treatments. The discontinuity in the
778 VEH-CNO line between ZT5-8 is because there were no sleep bouts during ZT6-7. Horizontal
779 bar denotes a significant effect of drug treatment and symbol above it indicates that the ALM-
780 CNO vs. VEH-CNO comparison was significantly different over this period ($p = 0.024$, $n = 10$, 2-
781 way repeated measures ANOVA, Bonferroni *post hoc t*-test). Arrows at the bottom left of the
782 abscissa in ***D*** and ***E*** indicate the times of dosing for VEH or ALM at ZT4 and for SAL or CNO at
783 ZT5. Symbols in ***B***, ***C*** and ***D*** denote significant differences between the indicated treatments (p
784 < 0.05) according to the legends in panels ***C*** and ***E*** when ANOVA revealed significant interaction
785 between drug treatment and power band.

786

787 **Figure 6**. Sparse activation of Hcrt and inhibitory neurons after CNO injection in *Gad2-IRES-*
788 *Cre;R26R-EYFP* mice. ***A***. Microphotographs showing hM3Dq-mCherry labeling in red (left), Hcrt
789 neurons in green (center), and the merged images (right) in *Gad2-IRES-Cre;R26R-EYFP* mice
790 transfected with AAV-TetO-hM3Dq-mCherry. White arrowheads denote Hcrt neurons co-
791 expressing hM3Dq-mCherry. Scale bar = 100 µm. ***B.*** Microphotographs showing Hcrt
792 immunostaining (left), c-FOS staining (center) and the merged images (right) in AAV-injected
793 *Gad2-IRES-Cre;R26R-EYFP mice.* White arrowheads denote Hcrt neurons that do not express c-
794 FOS. Scale bar = 50 µm. ***C***. Photomicrographs of DAB immunohistochemistry of transfected
795 neurons in LH (brown) and c-FOS expression (black nuclei) after SAL (upper panel) or CNO
796 (lower panel) injection. ***D***. Photomicrographs of GFP-labeled LH inhibitory neurons (green cells)
797 and c-FOS expression (black nuclei) in LH after SAL injection (upper panel) or CNO injection
798 (lower panel). All hypothalamic cells lateral to the dotted white line were included in the
799 Gad2/c-FOS counts. Scale bar denotes 50 µm. ***E***. GFP-labeled inhibitory neurons in the nRT
800 (green cells) and c-FOS expression (sparse black nuclei) after SAL injection (upper panel) or CNO
801 injection (lower panel). Scale bar = 100 µm (same scale as panel C).

802

803 **Figure 7.** c-FOS activity in the SuM does not increase after CNO treatment. ***A***. c-FOS expression
804 in the mammillary region after treatment with saline followed by 90 min of SD. ***B***. c-FOS
805 expression in the SuM after CNO treatment showing similar c-FOS expression than saline
806 treatment. ***C***. mCherry immunohistochemistry for the region depicted in ***B*** showing hM3Dq
807 expression only in the lateral regions and almost no labelling in the medial aspect of SuM. Black

dotted lines indicate the approximate region used for counting c-FOS in the SuM. LM, lateral mammillary nucleus; MM, medial mammillary nucleus. Scale bar denotes 250 μm.

Figure 8. Dietary DOX regulates Hcrt neuron transfection and duration of W promotion in *Orexin-tTA* mice. ***A, B***. Photomicrographs showing hM3Dq-mCherry labeling of transfected cells in red (left), Hcrt neurons in green (center), and the merged images (right) for *Orexin-tTA* mice in the DOX(+) (***A***) and DOX(-) (***B***) conditions. White arrows denote Hcrt neurons co-expressing hM3Dq-mCherry. Scale bar = 100 μm. ***C***, ***D***. Hourly percentage of time spent in W after injection of either VEH or ALM at ZT4 and either SAL or CNO at ZT5 in the DOX(+) (***C,*** $n = 11$) or DOX(-) (***D,*** $n = 13$) conditions. Symbols above each time point denote significant hourly differences ($p < 0.05$) between the indicated pairs of treatments according to the legends in panels ***A*** and ***B*** when a significant interaction between drug treatment and time was found ($p < 0.001$, 2-way repeated measures ANOVA, Bonferroni *post hoc t*-test). Arrows at the bottom left of the abscissa indicate the times of dosing for VEH or ALM at ZT4 and for SAL or CNO at ZT5. ***E***, ***F.*** Increase in total W time after dosing for ALM-CNO and VEH-CNO treatments relative to the VEH-SAL treatment in the DOX(+) (***E***, $p = 0.29$, *t*-test, $n = 11$) and DOX(-) (***F***, $p = 0.029$, *t*-test, $n = 13$) conditions.

826

827 # Tables

828 **Table 1.** Summary of experimental treatments

Experiment	Strain	Sex	N	Number of treatments	Circadian phase	Results
CNO effect	*Gad-Cre;R26R-EYFP*	M&F	9	2	active	Figs. 2 & 3
ALM effect	*Gad-Cre;R26R-EYFP*	M&F	9	2	active	Not shown
CNO control	C57BL/6J	M&F	8	2	inactive	Fig. 3***B***
ALM and CNO interaction	*Gad-Cre;R26R-EYFP*	M&F	10	4	inactive	Figs. 4 & 5
ALM and CNO interaction	*Orexin-tTA* (DOX+)	M	11	4	inactive	Fig. 8***C,E***
ALM and CNO interaction	*Orexin-tTA* (DOX-)	M	13	4	inactive	Fig. 8***D,F***

829 *All *Gad-Cre;R26R-EYFP mice were* $Cre^{+}/R26^{+}$ *except 1* $Cre^{+}/R26^{-}$ *male mouse.*

830

831 **Table 2.** Results of 2-way ANOVA for total increase in W time between DOX(+), DOX(-), ALM-

832 CNO and VEH-CNO drug treatment (Fig. 8).

Source	Sum Sq.	D.F.	Mean Sq.	*F*	*p*
Chow	15379.3	1	15379.3	5.11	0.035
Drug	16457.3	1	16457.3	5.47	0.0319
Chow*Drug	1138.4	1	1138.4	0.38	0.54
Error	132484.1	44	3011		
Total	166308.6	47			

833

834

References

Alam MA, Mallick BN (2008) Glutamic acid stimulation of the perifornical-lateral hypothalamic area promotes arousal and inhibits non-REM/REM sleep. Neurosci Lett 439:281-286.

Alam MN, Gong H, Alam T, Jaganath R, McGinty D, Szymusiak R (2002) Sleep-waking discharge patterns of neurons recorded in the rat perifornical lateral hypothalamic area. J Physiol 538:619-631.

Bender F, Gorbati M, Cadavieco MC, Denisova N, Gao X, Holman C, Korotkova T, Ponomarenko A (2015) Theta oscillations regulate the speed of locomotion via a hippocampus to lateral septum pathway. Nat Commun 6:8521.

Black SW, Morairty SR, Fisher SP, Chen TM, Warrier DR, Kilduff TS (2013) Almorexant promotes sleep and exacerbates cataplexy in a murine model of narcolepsy. Sleep 36:325-336.

Bonnavion P, de Lecea L (2010) Hypocretins in the control of sleep and wakefulness. Curr Neurol Neurosci Rep 10:174-179.

Cerri M, Del Vecchio F, Mastrotto M, Luppi M, Martelli D, Perez E, Tupone D, Zamboni G, Amici R (2014) Enhanced slow-wave EEG activity and thermoregulatory impairment following the inhibition of the lateral hypothalamus in the rat. PLoS One 9:e112849.

Dantz B, Edgar DM, Dement WC (1994) Circadian rhythms in narcolepsy: studies on a 90 minute day. Electroencephalogr Clin Neurophysiol 90:24-35.

de Lecea L, Kilduff TS, Peyron C, Gao X, Foye PE, Danielson PE, Fukuhara C, Battenberg EL, Gautvik VT, Bartlett FS, 2nd, Frankel WN, van den Pol AN, Bloom FE, Gautvik KM, Sutcliffe JG (1998) The hypocretins: hypothalamus-specific peptides with neuroexcitatory activity. Proc Natl Acad Sci U S A 95:322-327.

857 de Ryck M, Teitelbaum P (1978) Neocortical and hippocampal EEG in normal and lateral
858 hypothalamic-damaged rats. Physiol Behav 20:403-409.
859 Dittrich L, Morairty SR, Warrier DR, Kilduff TS (2015) Homeostatic sleep pressure is the primary
860 factor for activation of cortical nNOS/NK1 neurons. Neuropsychopharmacology 40:632-639.
861 Eriksson KS, Sergeeva OA, Selbach O, Haas HL (2004) Orexin (hypocretin)/dynorphin neurons
862 control GABAergic inputs to tuberomammillary neurons. Eur J Neurosci 19:1278-1284.
863 Gerashchenko D, Kohls MD, Greco M, Waleh NS, Salin-Pascual R, Kilduff TS, Lappi DA, Shiromani
864 PJ (2001) Hypocretin-2-saporin lesions of the lateral hypothalamus produce narcoleptic-like
865 sleep behavior in the rat. J Neurosci 21:7273-7283.
866 Hara J, Beuckmann CT, Nambu T, Willie JT, Chemelli RM, Sinton CM, Sugiyama F, Yagami K, Goto
867 K, Yanagisawa M, Sakurai T (2001) Genetic ablation of orexin neurons in mice results in
868 narcolepsy, hypophagia, and obesity. Neuron 30:345-354.
869 Herrera CG, Cadavieco MC, Jego S, Ponomarenko A, Korotkova T, Adamantidis A (2016)
870 Hypothalamic feedforward inhibition of thalamocortical network controls arousal and
871 consciousness. Nat Neurosci 19:290-298.
872 Hinman JR, Penley SC, Long LL, Escabi MA, Chrobak JJ (2011) Septotemporal variation in
873 dynamics of theta: speed and habituation. J Neurophysiol 105:2675-2686.
874 Kilduff TS, Peyron C (2000) The hypocretin/orexin ligand-receptor system: implications for sleep
875 and sleep disorders. Trends Neurosci 23:359-365.
876 Kornum BR, Knudsen S, Ollila HM, Pizza F, Jennum PJ, Dauvilliers Y, Overeem S (2017)
877 Narcolepsy. Nat Rev Dis Primers 3:16100.

878 Kosse C, Schone C, Bracey E, Burdakov D (2017) Orexin-driven GAD65 network of the lateral
879 hypothalamus sets physical activity in mice. Proc Natl Acad Sci U S A 114:4525-4530.
880 Koyama Y, Takahashi K, Kodama T, Kayama Y (2003) State-dependent activity of neurons in the
881 perifornical hypothalamic area during sleep and waking. Neuroscience 119:1209-1219.
882 Krolicki L, Chodobski A, Skolasinska K (1985) The effect of stimulation of the reticulo-
883 hypothalamic-hippocampal systems on the cerebral blood flow and neocortical and
884 hippocampal electrical activity in cats. Exp Brain Res 60:551-558.
885 Lee MG, Hassani OK, Jones BE (2005) Discharge of identified orexin/hypocretin neurons across
886 the sleep-waking cycle. J Neurosci 25:6716-6720.
887 Li FW, Deurveilher S, Semba K (2011) Behavioural and neuronal activation after microinjections
888 of AMPA and NMDA into the perifornical lateral hypothalamus in rats. Behav Brain Res
889 224:376-386.
890 McGregor R, Shan L, Wu MF, Siegel JM (2017) Diurnal fluctuation in the number of
891 hypocretin/orexin and histamine producing: Implication for understanding and treating
892 neuronal loss. PLoS One 12:e0178573.
893 Morairty SR, Dittrich L, Pasumarthi RK, Valladao D, Heiss JE, Gerashchenko D, Kilduff TS (2013) A
894 role for cortical nNOS/NK1 neurons in coupling homeostatic sleep drive to EEG slow wave
895 activity. Proc Natl Acad Sci U S A 110:20272-20277.
896 Morairty SR, Revel FG, Malherbe P, Moreau JL, Valladao D, Wettstein JG, Kilduff TS, Borroni E
897 (2012) Dual hypocretin receptor antagonism is more effective for sleep promotion than
898 antagonism of either receptor alone. PLoS One 7:e39131.

899 Nauta WJ (1946) Hypothalamic regulation of sleep in rats; an experimental study. J
900 Neurophysiol 9:285-316.
901 Pedersen NP, Ferrari L, Venner A, et al. Supramammillary glutamate neurons are a key node of
902 the arousal system. *Nat Commun*. 2017;8:1405.
903 Perez-Leighton C, Little MR, Grace M, Billington C, Kotz CM (2017) Orexin signaling in rostral
904 lateral hypothalamus and nucleus accumbens shell in the control of spontaneous physical
905 activity in high- and low-activity rats. Am J Physiol Regul Integr Comp Physiol 312:R338-
906 R346.
907 Peyron C, Tighe DK, van den Pol AN, de Lecea L, Heller HC, Sutcliffe JG, Kilduff TS (1998)
908 Neurons containing hypocretin (orexin) project to multiple neuronal systems. J Neurosci
909 18:9996-10015.
910 Qualls-Creekmore E, Yu S, Francois M, Hoang J, Huesing C, Bruce-Keller A, Burk D, Berthoud HR,
911 Morrison CD, Munzberg H (2017) Galanin-Expressing GABA Neurons in the Lateral
912 Hypothalamus Modulate Food Reward and Noncompulsive Locomotion. J Neurosci 37:6053-
913 6065.
914 Ranson SW (1939) Somnolence caused by hypothalamic lesions in monkeys. Arch
915 NeurolPsychiatr:1-23.
916 Saper CB, Scammell TE, Lu J (2005) Hypothalamic regulation of sleep and circadian rhythms.
917 Nature 437:1257-1263.
918 Sasaki K, Suzuki M, Mieda M, Tsujino N, Roth B, Sakurai T (2011) Pharmacogenetic modulation
919 of orexin neurons alters sleep/wakefulness states in mice. PLoS One 6:e20360.

920 Schone C, Apergis-Schoute J, Sakurai T, Adamantidis A, Burdakov D (2014) Coreleased orexin
921 and glutamate evoke nonredundant spike outputs and computations in histamine neurons.
922 Cell Rep 7:697-704.
923 Schone C, Cao ZF, Apergis-Schoute J, Adamantidis A, Sakurai T, Burdakov D (2012) Optogenetic
924 probing of fast glutamatergic transmission from hypocretin/orexin to histamine neurons in
925 situ. J Neurosci 32:12437-12443.
926 Shin J, Talnov A, Matsumoto G, Brankack J (2001) Hippocampal theta rhythm and running
927 speed: A reconsideration using within-single trial analysis. Neurocomputing 38:1567-1574.
928 Shoham S, Teitelbaum P (1982) Subcortical waking and sleep during lateral hypothalamic
929 "somnolence" in rats. Physiol Behav 28:323-333.
930 Sinnamon HM, Karvosky ME, Ilch CP (1999) Locomotion and head scanning initiated by
931 hypothalamic stimulation are inversely related. Behav Brain Res 99:219-229.
932 Tabuchi S, Tsunematsu T, Black SW, Tominaga M, Maruyama M, Takagi K, Minokoshi Y, Sakurai
933 T, Kilduff TS, Yamanaka A (2014) Conditional ablation of orexin/hypocretin neurons: a new
934 mouse model for the study of narcolepsy and orexin system function. J Neurosci 34:6495-
935 6509.
936 Taniguchi H, He M, Wu P, Kim S, Paik R, Sugino K, Kvitsiani D, Fu Y, Lu J, Lin Y, Miyoshi G, Shima
937 Y, Fishell G, Nelson SB, Huang ZJ (2011) A resource of Cre driver lines for genetic targeting of
938 GABAergic neurons in cerebral cortex. Neuron 71:995-1013.
939 Thannickal T, Moore R, Y., Nienhuis R, Ramanathan L, Gulyani S, Aldrich M, Cornford M, Siegel
940 JM (2000) Reduced number of hypocretin neurons in human narcolepsy. Neuron 27:469-
941 474.

942 Torrealba F, Yanagisawa M, Saper CB (2003) Colocalization of orexin a and glutamate
943 immunoreactivity in axon terminals in the tuberomammillary nucleus in rats. Neuroscience
944 119:1033-1044.
945 Vanderwolf CH (1969) Hippocampal electrical activity and voluntary movement in the rat.
946 Electroencephalogr Clin Neurophysiol 26:407-418.
947 Venner A, Anaclet C, Broadhurst RY, Saper CB, Fuller PM (2016) A Novel Population of Wake-
948 Promoting GABAergic Neurons in the Ventral Lateral Hypothalamus. Curr Biol 26:2137-
949 2143.
950 Von Economo C (1930) Sleep as a problem of localization. Journal of Nervous Mental
951 Disorders:249-259.
952
953

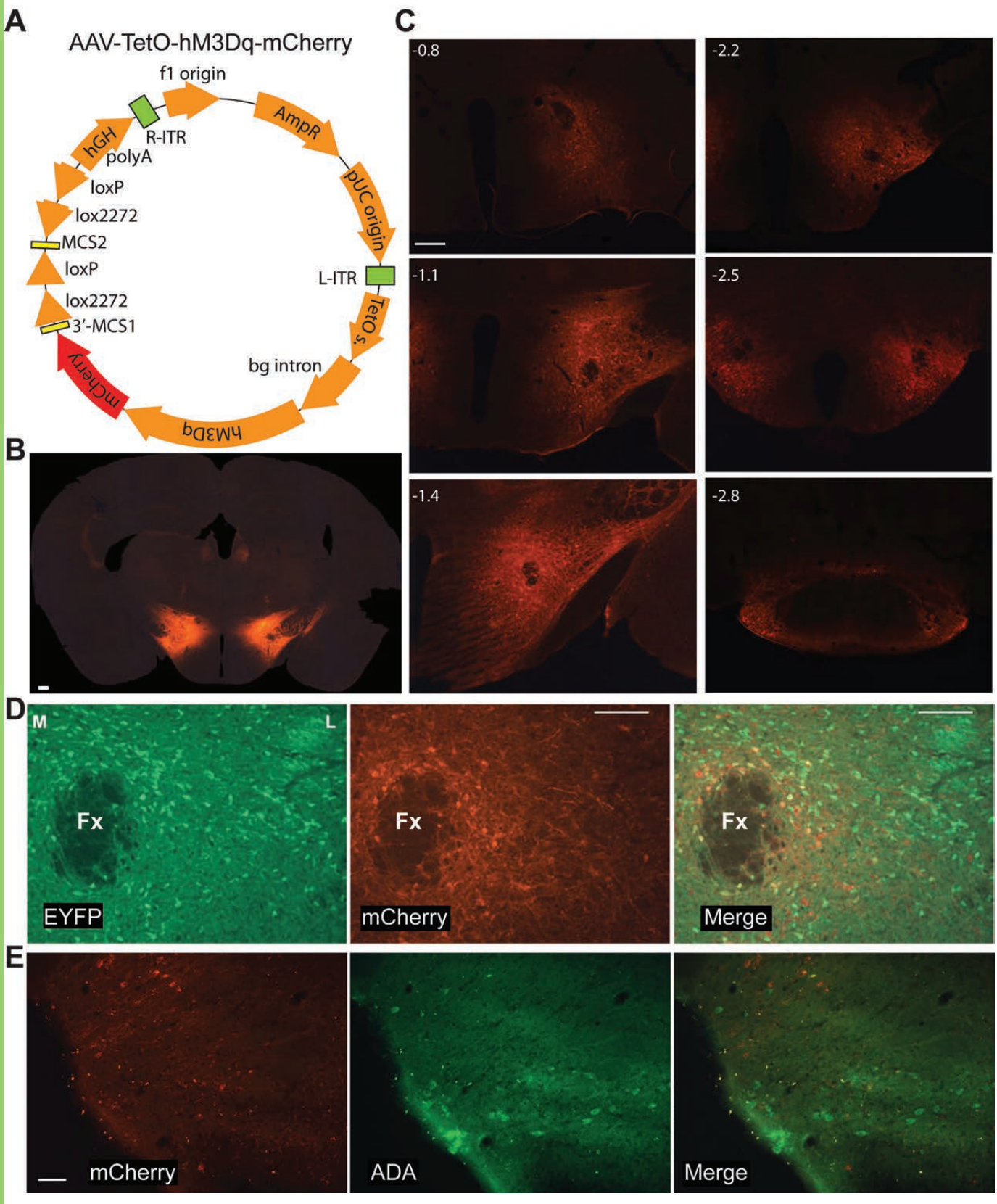

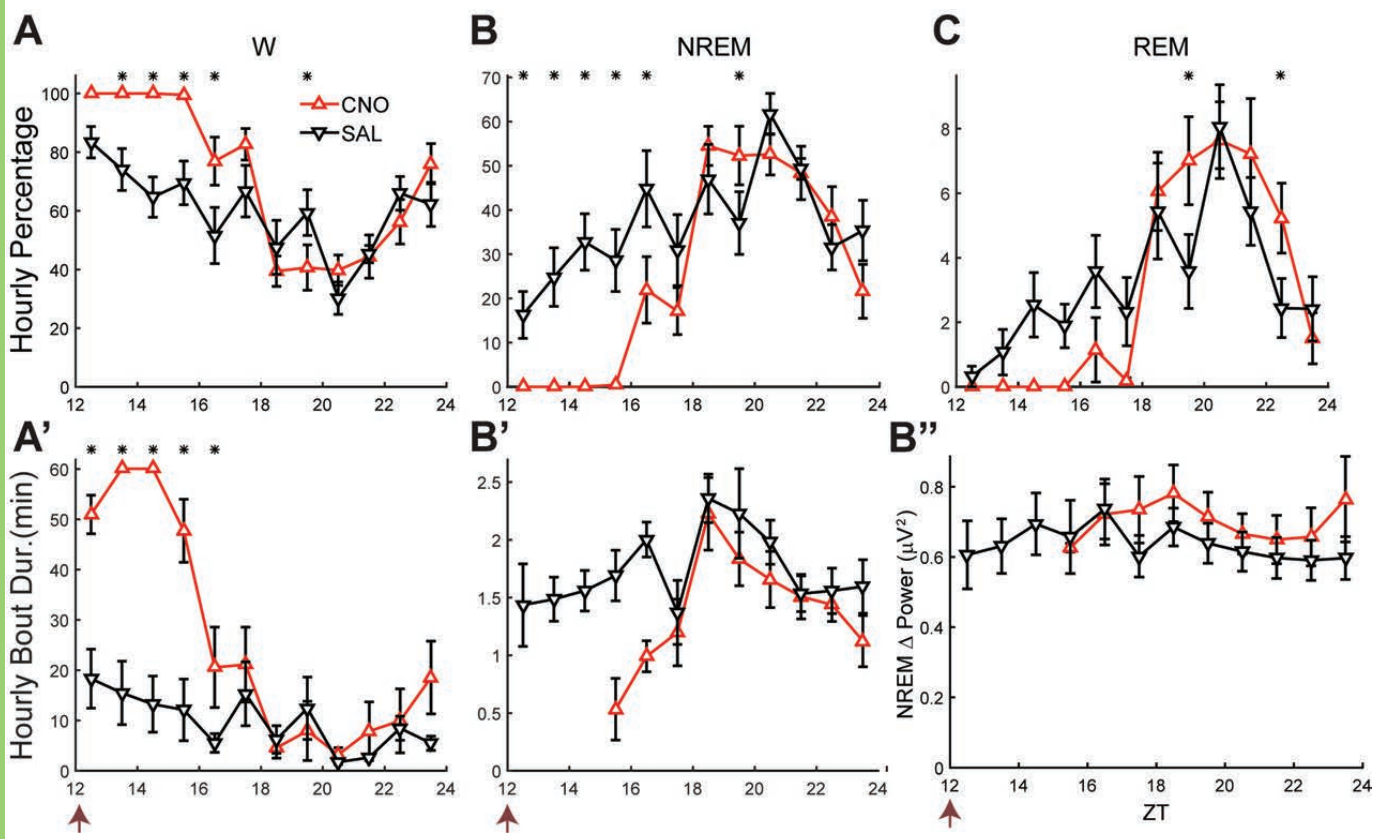

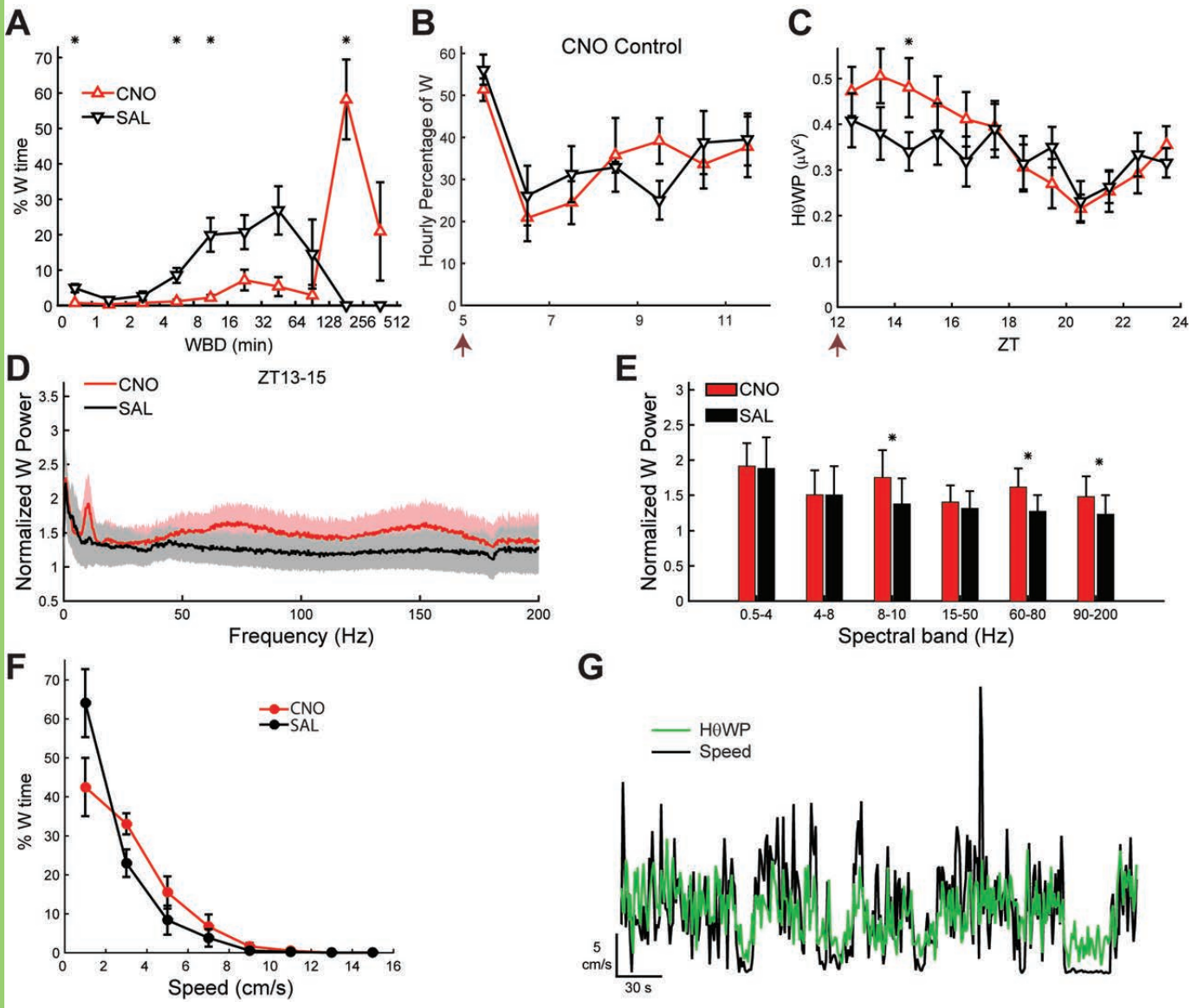

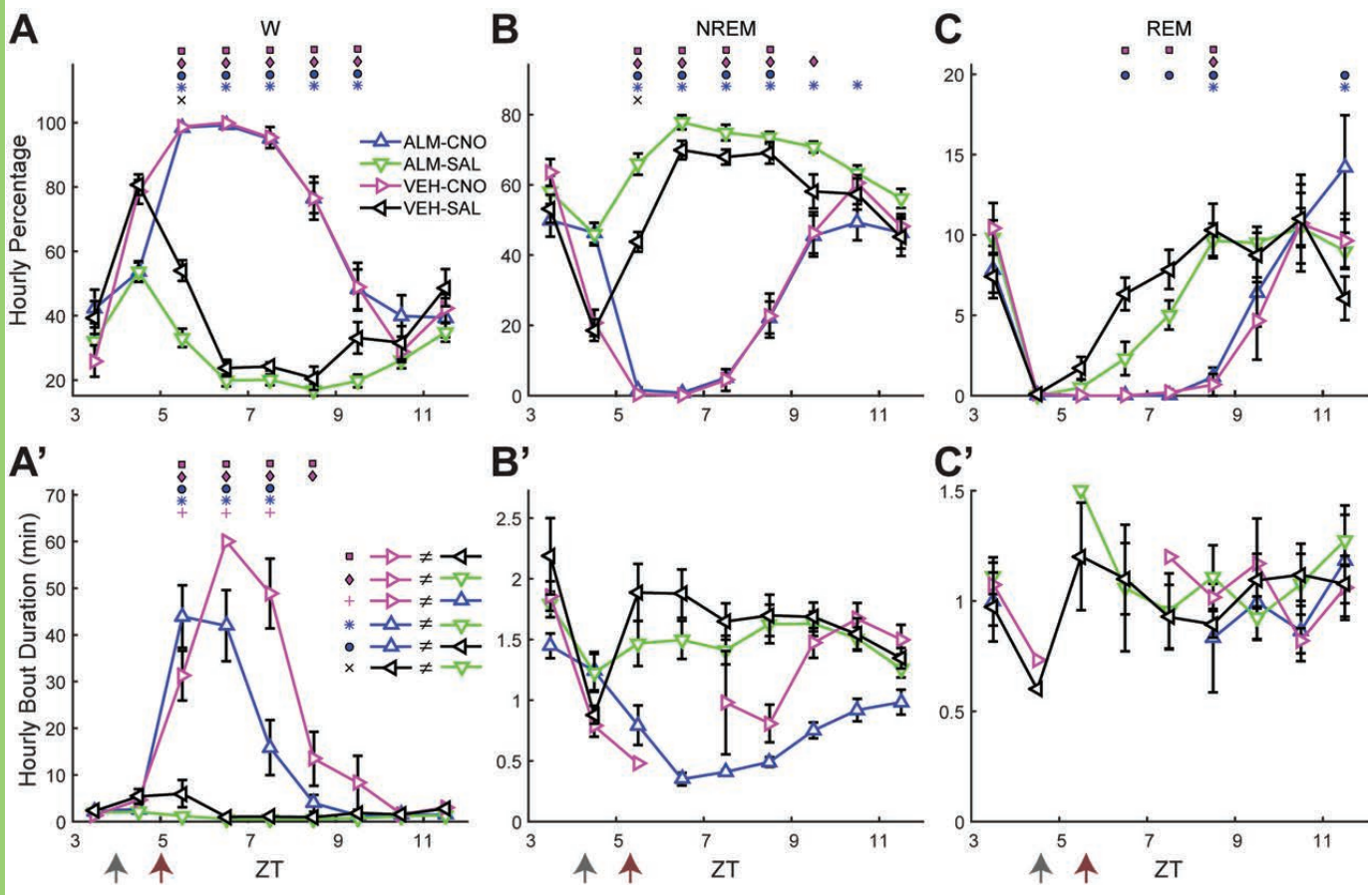

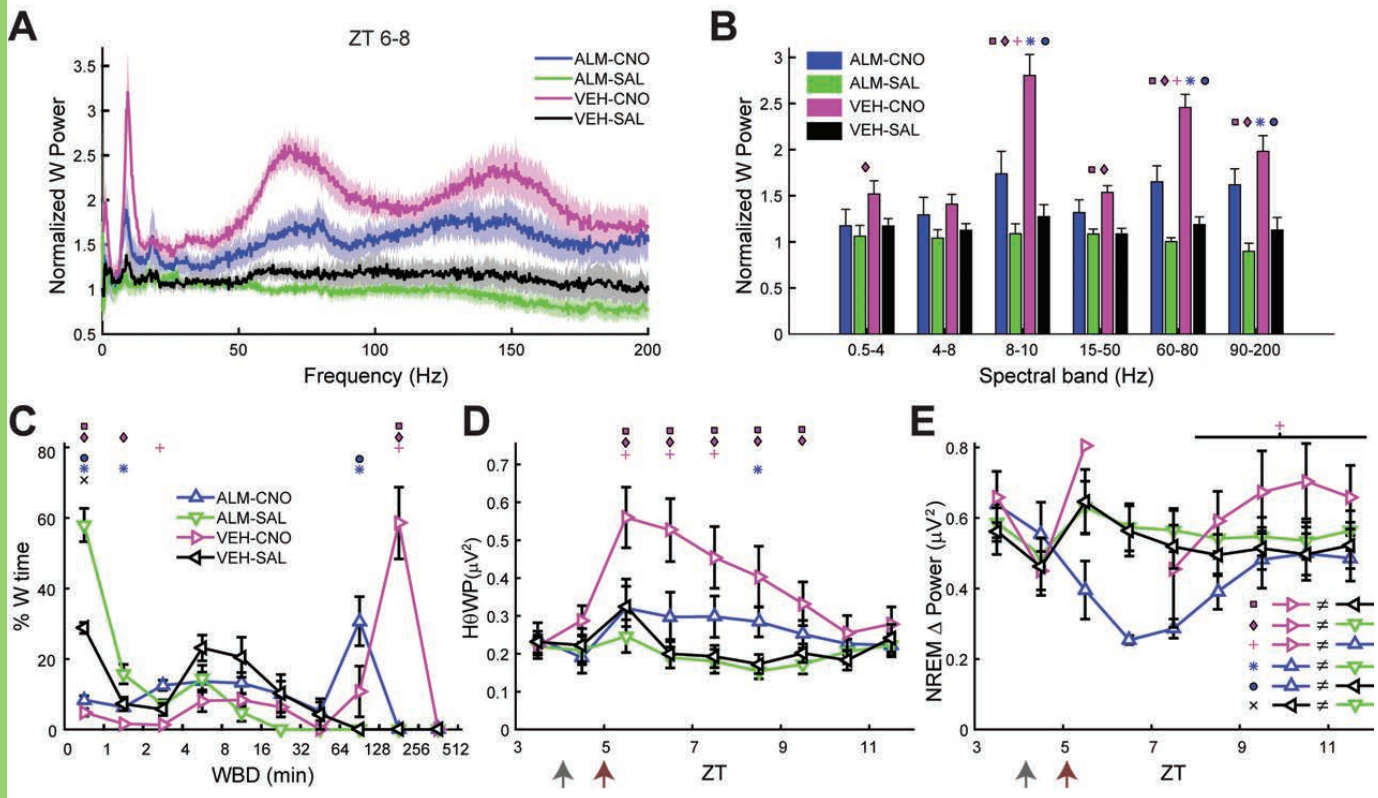

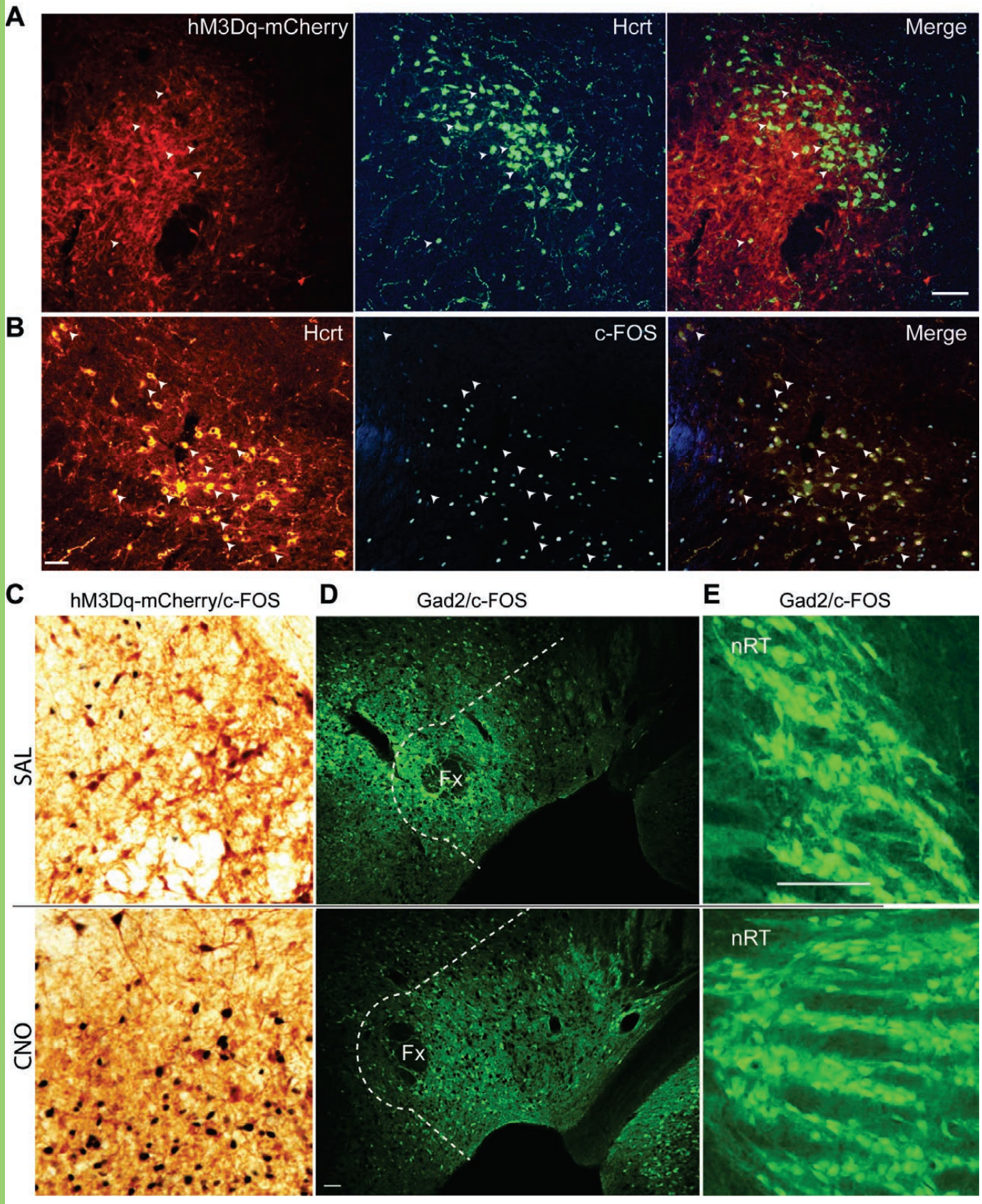

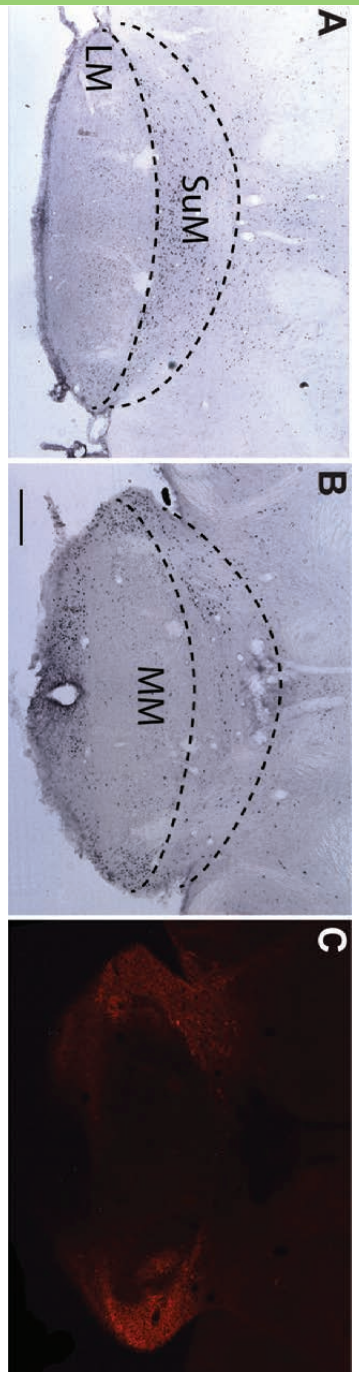

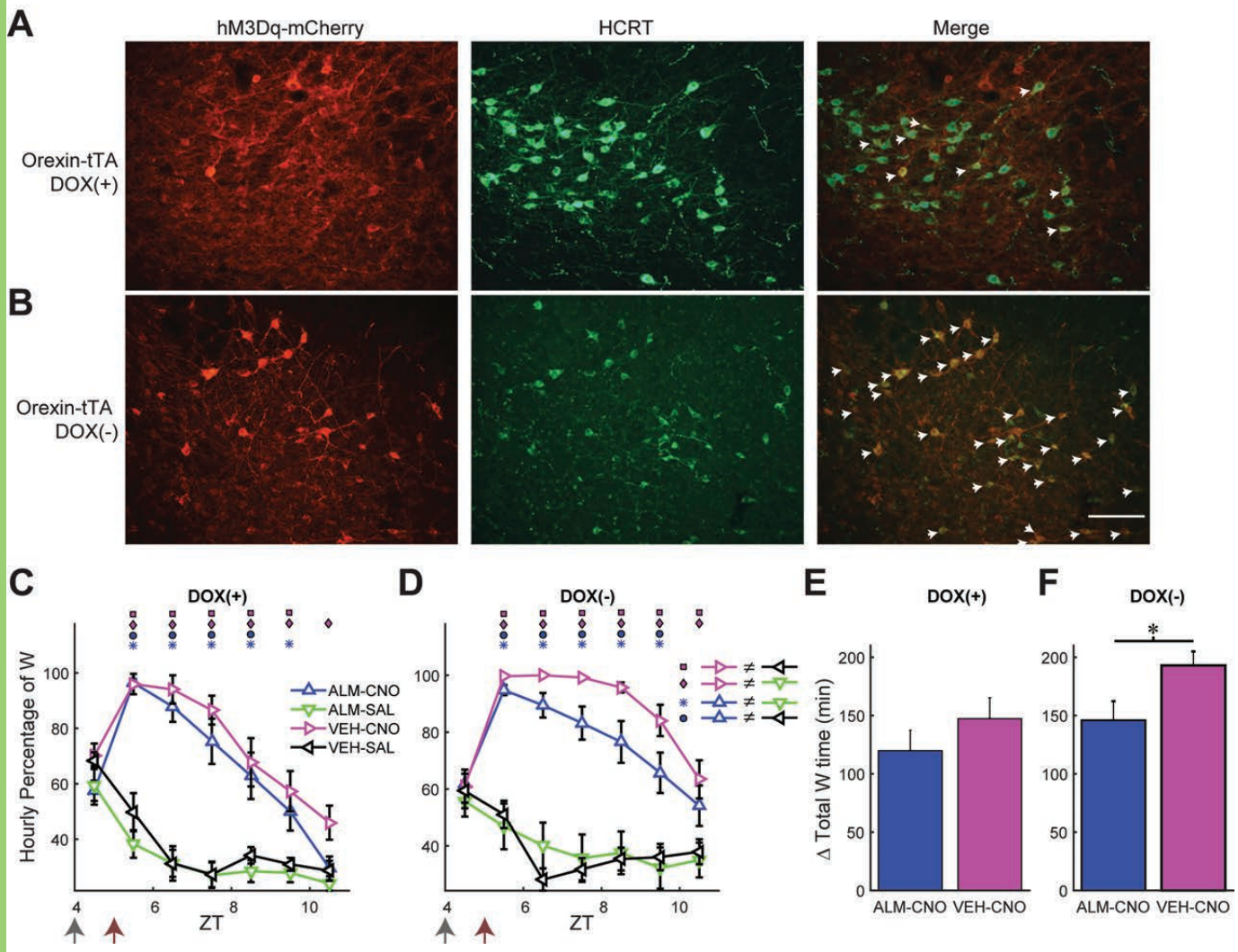

Table 1. Summary of experimental treatments

Experiment	Strain	Sex	N	Number of treatments	Circadian phase	Results
CNO effect	*Gad-Cre;R26R-EYFP*	M&F	9	2	active	Figs. 2 & 3
ALM effect	*Gad-Cre;R26R-EYFP*	M&F	9	2	active	Not shown
CNO control	C57BL/6J	M&F	8	2	inactive	Fig. 3***B***
ALM and CNO interaction	*Gad-Cre;R26R-EYFP*	M&F	10	4	inactive	Figs. 4 & 5
ALM and CNO interaction	*Orexin-tTA* (DOX+)	M	11	4	inactive	Fig. 7***C,E***
ALM and CNO interaction	*Orexin-tTA* (DOX-)	M	13	4	inactive	Fig. 7***D,F***

*All *Gad-Cre;R26R-EYFP mice were* $Cre^{+}/R26^{+}$ *except 1* $Cre^{+}/R26^{-}$ *male mouse.*

Table 2. Results of 2-way ANOVA for total increase in W time between DOX(+), DOX(-), ALM-CNO and VEH-CNO drug treatment.

Source	Sum Sq.	D.F.	Mean Sq.	*F*	*p*
Chow	15379.3	1	15379.3	5.11	0.035
Drug	16457.3	1	16457.3	5.47	0.0319
Chow*Drug	1138.4	1	1138.4	0.38	0.54
Error	132484.1	44	3011		
Total	166308.6	47			